RESEARCH REPORT

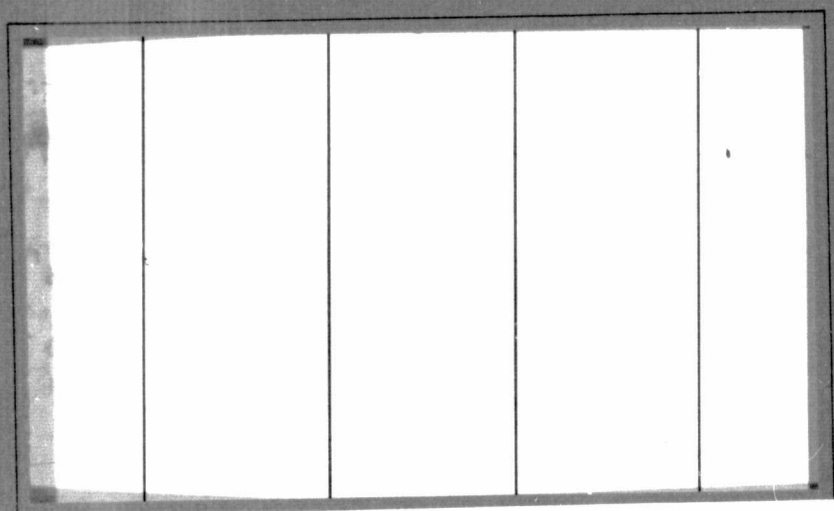

Battelle
Columbus Laboratories

FINAL REPORT

on

FUNDAMENTAL ANALYSIS OF THE FAILURE OF POLYMER-BASED FIBER REINFORCED COMPOSITES

September 30, 1975

by

M. F. Kanninen, E. F. Rybicki,
W. I. Griffith, and D. Broek

to

NATIONAL AERONAUTICS AND SPACE ADMINISTRATION
AMES RESEARCH CENTER
MOFFETT FIELD, CALIFORNIA

NASA-AMES GRANT NSG-2038

BATTELLE
Columbus Laboratories
505 King Avenue
Columbus, Ohio 43201

Battelle
Columbus Laboratories
505 King Avenue
Columbus, Ohio 43201
Telephone (614) 424-6424
Telex 24-5454

December 2, 1975

Mr. Dell Williams, Chief
Materials Research Branch
NASA-Ames Research Center
Moffett Field, California 94035

Dear Dell:

Enclosed are three (3) copies of a final report on a "Fundamental Analysis of the Failure of Polymer-Based Fiber Reinforced Composites". This work was performed under subcontract to Virginia Polytechnic Institute and State University on NASA-Ames Grant NSG-2038. Please send me the names of other people that you think may want a copy.

We very much enjoyed working on this challenging technical problem. We look forward to furthering our work in this area and to continuing our association with you.

Sincerely,

Mel

M. F. Kanninen
Senior Researcher
Applied Solid Mechanics

MFK/cns

Enclosures

cc: NASA Scientific and Technical
Information Facility (2) ✓

Professor H. F. Brinson (1)

ABSTRACT

A mathematical model is being developed that will permit predictions of the strength of fiber reinforced composites containing known flaws to be made from the basic properties of their constituents. The approach is to embed a local heterogeneous region (LHR) surrounding the crack tip into an anisotropic elastic continuum. The intent is to have the model (1) permit an explicit analysis of the micromechanical processes involved in the fracture process, and (2) remain simple enough to be useful in practical computations. Material properties used in the analysis are to be obtained from a concurrent experimental program being carried out at Virginia Polytechnic Institute and State University.

Computations for arbitrary flaw size and orientation under arbitrary applied load combinations have been performed for unidirectional composites with linear elastic-brittle constituent behavior. The mechanical properties were nominally those of graphite epoxy. With the rupture properties arbitrarily varied to test the capability of the model to reflect real fracture modes in fiber composites, it is shown in the report that fiber breakage, matrix crazing, crack bridging, matrix-fiber debonding, and axial splitting can all occur during a period of (gradually) increasing load prior to catastrophic fracture. Of most importance, the computations reveal qualitatively the sequential nature of the stable crack growth process that precedes fracture in composites. Quantitative comparisons with the VPISU experimental results on edge-notched unidirectional graphite epoxy specimens have also been made and were found to be in fair agreement.

TABLE OF CONTENTS

LIST OF TABLES

LIST OF FIGURES

FUNDAMENTAL ANALYSIS OF THE FAILURE OF POLYMER-BASED FIBER REINFORCED COMPOSITES

INTRODUCTION

There are many different ways in which a structure made of a fiber reinforced composite material can become unable to adequately perform its primary function. In each such instance failure is considered to have occurred. The possible failure modes therefore encompass a wide range of possibilities from simple loss of structural rigidity due to gross inelastic deformation (e.g., yielding), through a reduction in load-carrying capacity due to localized damage or separation (e.g., interply delamination), to the complete loss of strength due to large-scale crack growth and fracture. Each of these failure modes can be gradual or rapid depending on the nature of the applied loads, the material properties, the geometry of the structure, and the presence of cracks or flaws. For polymer-based composites, the loading rate, the temperature, and previous load history can also play prominent roles.

In the work described in this report, emphasis is placed upon fracture and, therefore, the work will be primarily concerned with the "strength" of fiber composites containing known flaws. The term strength is conventionally taken to mean the load level at which failure occurs in a standard test specimen. Clearly, the strength will be a function of many different parameters arising in the test program and may or may not be directly applicable to engineering design situations. The primary purpose of the research described in this report is to provide a bridge between standard laboratory test procedures and actual engineering applications of fiber composites that will allow accurate reliable estimates of the failure loads for aircraft and other engineering structures. Such a capability does not presently exist.

The design tool that should be developed for the safe and efficient utilization of composite materials is a predictive capability for fracture that can take account of the applied loading, the geometry of the structure, and the environmental effects in terms of readily measurable properties of the composite's constituents and of its microstructural design. The primary benefits accruing from such an analytical capability are twofold. First, for a given structure, material, and load, the critical flaw size and type in a structural component can be estimated for comparison with actual flaws observed in an inspection program. Second, guidelines can be provided for the designer to tailor more fracture resistant "tougher" materials for specific engineering applications.

PROGRAM PLAN AND SUMMARY OF PROGRESS

The work described in this report represents the first year of effort in what is planned as a multiyear program. The specific objective of the first year's work was to develop the basic mathematical procedures required for the analysis model. To implement this work, attention was focussed on unidirectional composites with linear elastic-brittle material behavior. In subsequent work, the model will be extended to treat angle ply laminates and will include further refinements (e.g., inelastic constituent behavior) required in order to treat actual engineering problems.

The primary objective of the work will be achieved only if the mathematical model developed is capable of delineating the role of the various micromechanical failure processes that dictate the ultimate failure point of fiber reinforced composites. The research described in this report seeks this end by merging a micromechanical failure analysis with a macromechanical fracture mechanics approach. This approach treats the material as heterogeneous and anisotropic where microstructural effects predominate and as homogeneous and anisotropic where it is permissible and practical to do so. In this way, direct consideration can be given to

- The external size and shape of the structure and the laminate stacking sequence
- The applied loads acting on the structure, both mechanical and thermal, and environmental effects
- The size, shape, and orientation of a flaw in the laminate.

In particular, the manner in which these parameters influence the sequence of microstructural failure events whereby a flaw extends stably under an increasing load up to the point of catastrophic fracture will be determined. It should be understood that the conventional approach to fracture analysis, linear elastic fracture mechanics, is not capable of coping with this degree of complexity, thus necessitating the more general development being pursued here.

Linear elastic fracture mechanics (LEFM) is a predictive technique applicable to structural components containing crack-like flaws when the material used fits certain key assumptions used in the LEFM theory. Specifically, the material must behave very nearly as would a completely linear elastic perfectly homogeneous ideal material. The LEFM approach has been successful when properly applied (e.g., to high strength steel), but considerably less successful in applications where the basic assumptions are not well satisfied. Fiber reinforced composite materials are an outstanding example of the latter case. In particular, in fiber composites with a flaw, a nonlinear "damage" zone is generally produced at the flaw. This zone, generally growing in a stable manner under an increasing applied load, has a profound effect on the eventual point of complete fracture. This is shown, for example, in the work of Mandell, et al. [1]* as well as by many other investigators.

The damage zones in a fiber composite are the result of a large number of discrete failure processes, e.g., fiber breaking, matrix yielding, etc., that occur in the highly stressed region ahead of a crack-like flaw. These individual micromechanical events do not conform to the basic assumptions of LEFM. Consequently, it is not surprising that the agregate of such processes cannot be treated by LEFM. What is therefore needed is a generalized fracture mechanics treatment which explicitly recognizes the fundamental nature of damage growth in composite materials. Specifically, a proper analysis of fracture in fiber composites must be cognizant of two key features: the generally anisotropic constitutive behavior of the material, and the heterogeneous nature of the fracture process.

The approach developed in this report can be likened conceptually to boundary layer theory and, in application, to the well-established singular perturbation and matched asymptotic expansion techniques of fluid mechanics. That is, the problem of a composite material containing a flaw is divided into distinct "inner" and "outer" regions. In each of these regions, the material is modeled in different ways. The inner region, which contains the crack tip, is considered on the microscopic level and treats the material as being heterogeneous. The outer region surrounds the crack tip region. It is treated as a homogeneous orthotropic continuum. For simplicity, the inner crack tip region will be referred to in this report as the LHR (for local heterogeneous region) while the outer region will be simply called the continuum.

---

* References are given on page 45.

The LHR consists of elements representing the matrix, the fibers, and the fiber-matrix interface zones. The constitutive relations of these elements, up to and including their rupture points, are presumed to be known from experiments. Any element of a fiber composite ruptures when an intrinsic critical energy dissipation rate can be provided at some point of that element. These critical values are assumed to be independent of the local stress field environment at the point of incipient rupture. This permits data from fracture tests on isolated fibers, matrix material, and, possibly, unflawed composites (to obtain interface strengths) to be directly inserted into the model. Material properties used in the analysis work and, ultimately, critical tests of the predictions of the model will be obtained from a concurrent experimental program being carried out under NASA sponsorship at Virginia Polytechnic Institute and State University.

Progress to date has permitted computations to be performed for unidirectional composites with elastic-perfectly brittle constituent behavior. The mechanical properties have been those of graphite epoxy. The rupture properties have also been arbitrarily varied to test the capability of the model to reflect real fracture modes in fiber composites. It has been shown that fiber breakage, crack bridging, matrix-fiber debonding, and axial splitting can all occur during a period of (gradually) increasing load prior to catastrophic fracture. In this way, the sequential and interrelated manner in which each individual local rupture event occurs during damage growth preceding fracture in fiber composites is revealed by the computations.

Before beginning a detailed discussion of the analysis technique, it may be useful to briefly consider an overview of the entire program required to completely develop the analysis model. A tentative schedule to carry the development of the model from this, the first year, to the point where actual design problems with composite materials can be addressed is shown in Table I. The level of effort envisioned to complete these tasks is roughly the same for each year. Note that although a capability for treating fatigue crack growth will not be addressed until the third year of the program, it was thought desirable to begin to study the literature on the subject now. The resulting critical survey is given as Appendix A of this report. Similarly, in anticipation of contrasting the model developed in this work with others that have been offered, a discussion of experimentally observed failure mechanisms in composites and of various alternative analysis models for predicting fracture of composite materials is included as Appendix B.

TABLE I. TENTATIVE SCHEDULE FOR A PROGRAM LEADING TO A COMPLETE ANALYSIS MODEL OF POLYMER-BASED FIBER COMPOSITES WITH FLAWS

Time	Task	Objectives	Goals
First year[(a)]	Develop mathematical basis for prediction of damage growth in a LHR at the tip of a crack in plane deformation.	Demonstrate and verify practicability of the basic approach.	Perform computations for unidirectional flawed fiber composites for elastic-perfectly brittle constituent behavior.
Second year	Develop mathematical basis for model of angle ply laminates with arbitrary flaws.	Demonstrate and verify applicability of model to engineering structures.	Perform computations for multidirectional laminated plates with through-the-thickness cracks.
Third year	Develop mathematical basis for time-dependent loading and inelastic constituent behavior.	Demonstrate and verify use of the model under loads representative of service conditions.	Perform computations for fracture and fatigue with realistic material behavior.
Fourth year	Develop mathematical basis for dynamic and thermal material response with viscoelastic/plastic constituent behavior.	Demonstrate and verify use of the model under arbitrary service conditions.	Perform computations for fracture under impact loading and thermal shock; for fatigue crack growth under variable rate loading.

(a) Work performed at Battelle's Columbus Laboratories for NASA, Ames Research Center, through Virginia Polytechnic Institute and State University, 1974-75, as described in this report.

DESCRIPTION OF THE ANALYSIS TECHNIQUE

In the preceding section of this report, the objectives of the work and an outline of the general approach were given. The focal point for this description was the two-dimensional local heterogeneous region (LHR) surrounding the crack tip. A typical LHR model is shown in Figure 1. Depicted is a unidirectional fiber composite containing three distinct components: the fibers, the matrix, and the fiber-matrix interface zones. In this section of the report, the discrete elements that comprise the LHR and the manner in which they are assembled to give a quantitative predictive capability for composite fracture will be described in detail.

LHR Boundary Conditions

In the work performed so far, the interaction between the LHR and the continuum, as is appropriate for preliminary stages of the work, has been taken in the simplest possible manner. This is by specifying the displacements on the boundary of the LHR in accord with the "rigid boundary conditions" approach. Use of this scheme is tantamount to assuming that the LHR is large enough that the nonlinear inhomogeneity of the crack tip region does not affect the periphery of this region. In other words, the LHR and the continuum are assumed to be uncoupled. Consequently, the displacements at the LHR boundary are exactly the same as if the entire cracked body is an elastic continuum. The required relations can therefore be obtained from the work of Sih and Liebowitz [2]. Their approach is briefly summarized, as follows.

Consider a plate with its major dimensions lying in the xy plane. For either plane stress or plane strain deformation, the inplane strains ε_x, ε_y, and γ_{xy} will depend only on the inplane stresses σ_x, σ_y, and τ_{xy}. Hence, the appropriate constitutive relations for a rectilinearly anisotropic body in a state of plane deformation are given by

$$\begin{aligned}
\varepsilon_x &= a_{11}\sigma_x + a_{12}\sigma_y + a_{16}\tau_{xy} \\
\varepsilon_y &= a_{12}\sigma_x + a_{22}\sigma_y + a_{26}\tau_{xy} \\
\gamma_{xy} &= a_{16}\sigma_x + a_{26}\sigma_y + a_{66}\tau_{xy}
\end{aligned} \tag{1}$$

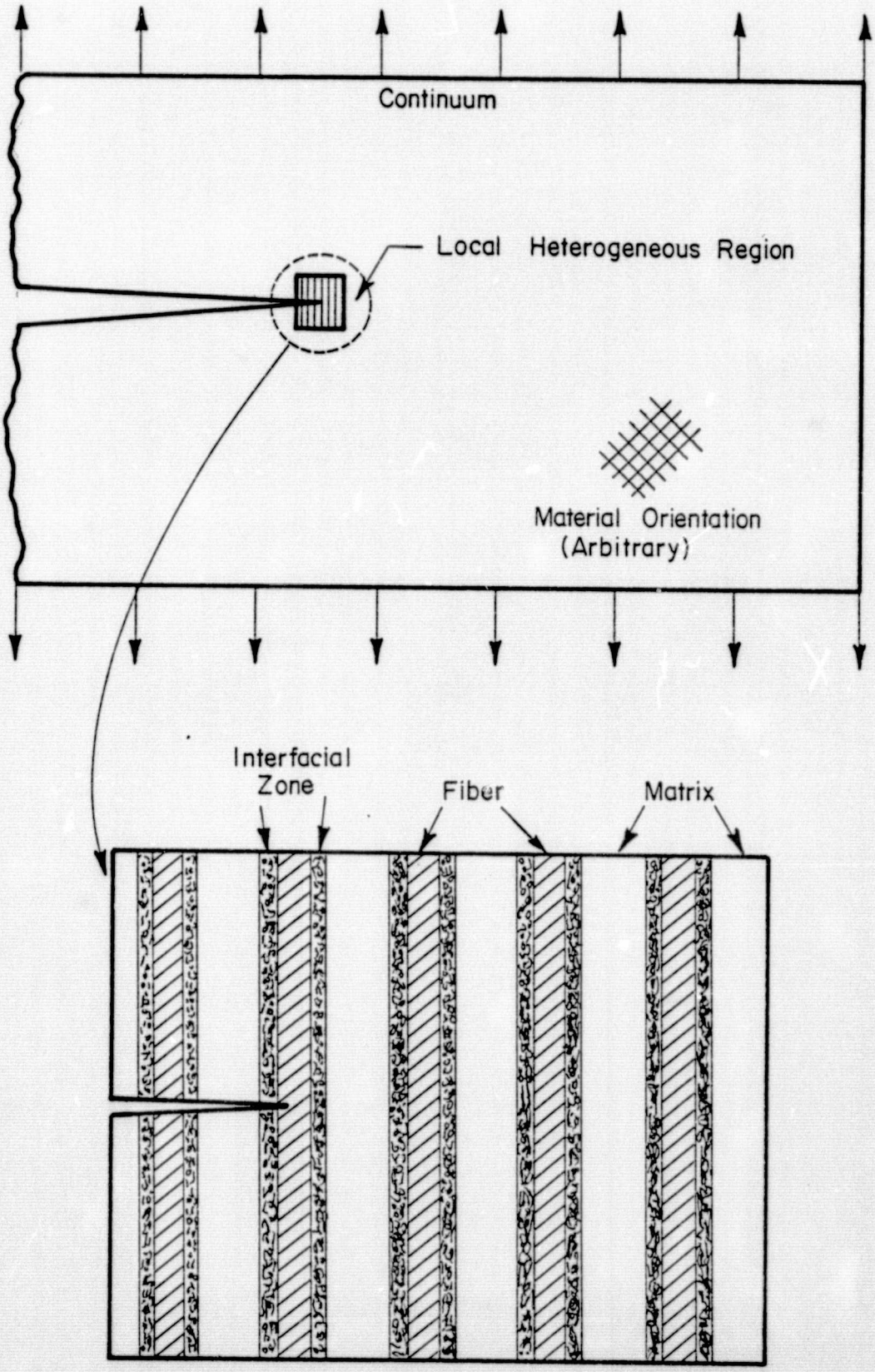

FIGURE 1. THE LHR CONCEPT

Sih and Liebowitz show that the solution to the governing differential equation of two-dimensional anisotropic elasticity theory is associated with the roots of the characteristic equation

$$a_{11}\,s^4 - 2a_{16}s^3 + (2a_{12} + a_{66})\,s^2 - 2\,a_{26}\,s + a_{22} = 0\ . \qquad (2)$$

It can be shown that the roots of Equation (2) are either complex or are pure imaginary. Hence, these can be labeled s_1, s_2, $\bar{s}_1$, and $\bar{s}_2$. This suggests the introduction of the complex variables $z_1 = x + s_1 y$ and $z_2 = x + s_2 y$. The plane problem of an anisotropic body is thereby reduced to the determination of two complex potential functions of a complex variable $\phi(z_1)$ and $\psi(z_2)$ that satisfy the prescribed boundary conditions of the problem.

As further shown in reference 2, the displacement field is expressed in terms of the potential functions by the relations

$$\begin{aligned} u &= 2\,Re\,\{p_1\,\phi(z_1) + p_2\,\psi(z_2)\} \\ v &= 2\,Re\,\{q_1\,\phi(z_1) + q_2\,\psi(z_2)\} \end{aligned} \qquad (3)$$

where u and v are the x and y displacement components and

$$p_1 = a_{11}\,s_1^2 + a_{12} - a_{16}\,s_1 \quad , \quad p_2 = a_{11}\,s_2^2 + a_{12} - a_{16}\,s_2$$

$$q_1 = \frac{1}{s_1}\,(a_{12}\,s_1^2 + a_{22} - a_{26}\,s_1) \ , \quad q_2 = \frac{1}{s_2}\,(a_{12}\,s_2^2 + a_{22} - a_{26}\,s_2)\ .$$

Omitting the details, potential functions for a cracked body infinite in extent have been determined for insertion into Equations (3). In particular, a solution for remote loading consisting of a uniform tensile loading σ acting in the direction normal to the crack plane and a shear loading τ parallel to the crack

plane for a crack of length $2a$ can be obtained. For a polar coordinate system with origin at the crack tip as shown in Figure 2, the displacements near the crack tip are given by

$$u = K_I\left(\frac{2r}{\pi}\right)^{1/2} \mathrm{Re}\left\{\frac{1}{s_2-s_1}\left[s_1 p_2 (\cos\phi + s_2 \sin\phi)^{1/2} + \right.\right.$$

$$\left.\left. - s_2 p_1 (\cos\phi + s_1 \sin\phi)^{1/2}\right]\right\} +$$

$$+ K_{II}\left(\frac{2r}{\pi}\right)^{1/2} \mathrm{Re}\left\{\frac{1}{s_1-s_2}\left[p_2 (\cos\phi + s_2 \sin\phi)^{1/2} + \right.\right.$$

$$\left.\left. - p_1 (\cos\phi + s_1 \sin\phi)^{1/2}\right]\right\} \qquad (4)$$

and

$$v = K_I\left(\frac{2r}{\pi}\right)^{1/2} \mathrm{Re}\left\{\frac{1}{s_1-s_2}\left[s_1 q_2 (\cos\phi + s_2 \sin\phi)^{1/2} + \right.\right.$$

$$\left.\left. - s_2 q_1 (\cos\phi + s_1 \sin\phi)^{1/2}\right]\right\} +$$

$$+ K_{II}\left(\frac{2r}{\pi}\right)^{1/2} \mathrm{Re}\left\{\frac{1}{s_1-s_2}\left[q_2 (\cos\phi + s_2 \sin\phi)^{1/2} + \right.\right.$$

$$\left.\left. - q_1 (\cos\phi + s_1 \sin\phi)^{1/2}\right]\right\} , \qquad (5)$$

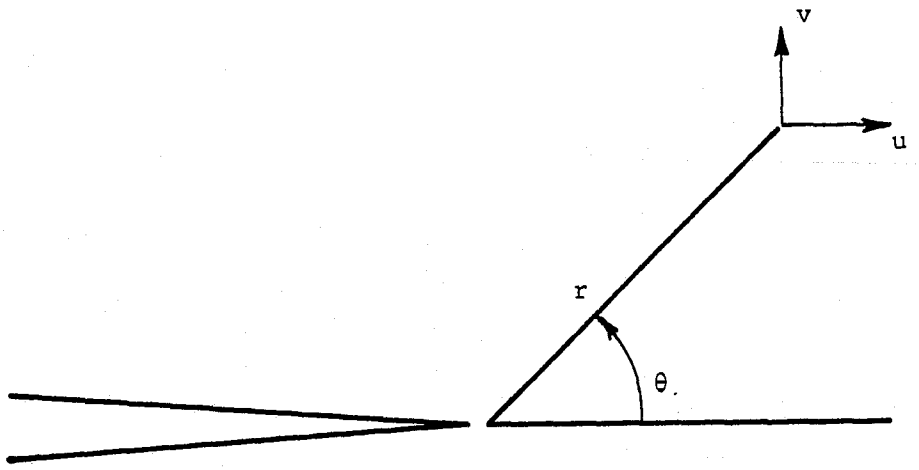

FIGURE 2. DISPLACEMENT COMPONENTS FOR A POINT IN THE VICINITY OF THE CRACK TIP

where

$$K_I = \sigma \sqrt{\pi a}$$

and (6)

$$K_{II} = \tau \sqrt{\pi a}$$

are the Mode I and Mode II stress-intensity factors for the problem.

Equations (4) and (5) can be used to determine displacements on the LHR boundary via the rigid boundary-condition approach. This means that the applied stresses acting on the body are transmitted through the continuum region to the crack-tip region and are "sensed" at the crack tip in terms of the stress-intensity factors K_I and K_{II}. An independent specification of the load and crack length is therefore unnecessary. Hence, although derived for an infinite medium, the approach can be used for bodies with finite boundaries by simply inserting the appropriate stress-intensity factors. In doing this, it must be tacitly assumed that the LHR is (1) large enough relative to the microstructural dimensions of the composite that the boundary displacements are closely given by continuum theory and (2) small enough relative to the crack length and dimensions of the body that the singular behavior of the continuum solution at the crack tip dominates.

While appropriate for preliminary work, it is anticipated that the rigid boundary condition approach--even with periodic updating to reflect the progress of the crack through the LHR--may prove to be too restrictive. Therefor, in subsequent work, a flexible boundary-condition approach which extends an approach developed in work previously carried out at Battelle [3] will be used. This is described in more detail in the Recommended Further Research section of this report. It might be noted that with flexible boundary conditions, crack length and load must be specified individually.

The LHR Element

As shown in Figure 1, the LHR for a fiber reinforced composite is considered to be made up of three different types of constituents: fiber, matrix, and fiber-matrix interface. Each of the individual constituents in the LHR must be capable of rupturing to allow the body to exhibit the changes in strength that correspond to various levels and orientations of local breakage. A good deal of success has been obtained by Kanninen [4,5] using "spring-like" elements to model a local fracture phenomena. This fact, taken together with the increased computational simplicity of this approach, has led to the adoption of the basic element shown in Figure 3 for this work.

As shown in Figure 3, each element has eight degrees of freedom and is connected in the LHR at its four corner node points. Extensional stiffness is provided by four extensional connectors. These connectors resemble simple extensional springs, but also have a lateral contraction or Poisson effect. A material made up of a set of these connectors behaves in uniform extension exactly like a homogeneous orthotropic material. Similarly, shear stiffness is incorporated in the element through a rotary spring at each node point to give the proper response to shear loadings. The values of the spring constants are functions of the material's elastic constants and of the element size and shape.

In addition to giving the proper response to loads, the LHR elements fracture according to the "codes" shown in Figure 4. In Figure 4, Fracture Code 1 represents an increment of crack extension in the plane lying midway between Nodes 1 and 4 that extends from the left side of the element to the center of the element. Fracture Code 2 represents the continuation of the crack to the right side of the element. Fracture Codes 3 and 4 represent similar increments of cracking in the vertical direction.

Using an energy approach, it is possible to trace those components of the elemental stiffness matrix that are associated with each fracture code in every element in the LHR. This information can be assembled into the stiffness matrix such that a solution can be obtained for the incipient rupture of any subelement in the LHR. Note that this is most easily possible if (as in the present work), the constituent behavior is restricted to being linear elastic to the rupture point. Inelastic behavior, while more complicated, is not precluded, however.

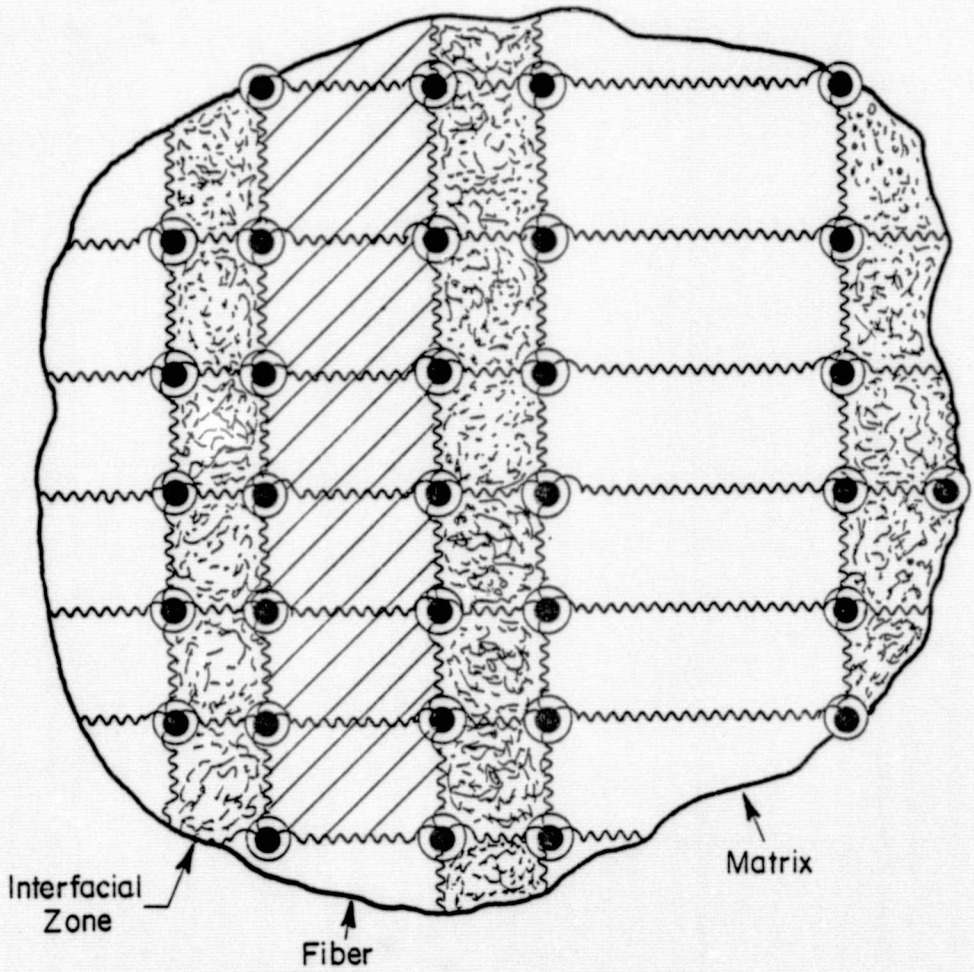

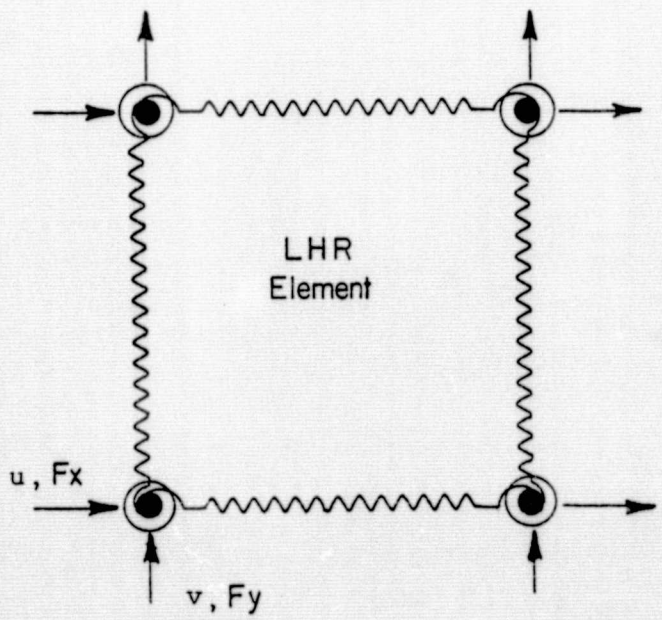

FIGURE 3. DETAILED REPRESENTATION OF AN LHR ELEMENT

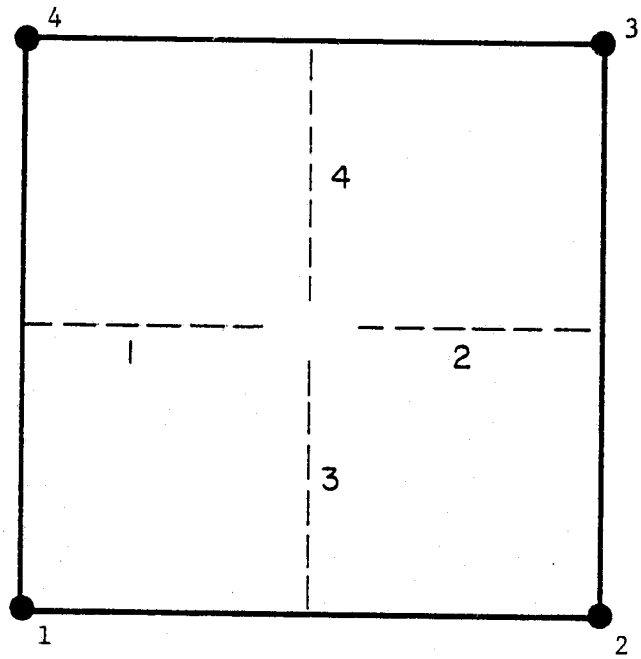

FIGURE 4. THE FRACTURE CODES CONTAINED IN AN LHR ELEMENT

Knowledge of the stiffness components attributable to each fracture condition also provides a method of calculating the energy-release rate for crack advance by any of the four codes provided for in each LHR element. Of course, the critical rupture energy values must be specified to provide a decision rule for breakage in each separate element. Note that while the model allows separate critical values to be specified for each of the four fracture codes for every one of the elements in the LHR, ordinarily different values will be specified only for the different constituents, i.e., fiber, matrix, or interface.

Elemental Stiffness Formulation

Energy principles can conveniently be used to determine the stiffness of the LHR structure. The sign conventions for an LHR element will be taken as shown in Figure 5. Then, using the following notation:

C_i = rotational spring constant at the $i^{\underline{th}}$ node

K_{xx}^{ij} = extensional stiffness in the x direction between the $i^{\underline{th}}$ and $j^{\underline{th}}$ nodes

K_{yy}^{ij} = extensional stiffness in the y direction between the $i^{\underline{th}}$ and $j^{\underline{th}}$ nodes

K_{xy}^{ij} = cross extensional component (effect of Poisson's ratio) between the $i^{\underline{th}}$ and $j^{\underline{th}}$ nodes

u_i = x displacement at the $i^{\underline{th}}$ node

v_i = y displacement at the $i^{\underline{th}}$ node,

the total strain energy U stored in the element for any set of arbitrary nodal displacements u_i and v_i can be written as

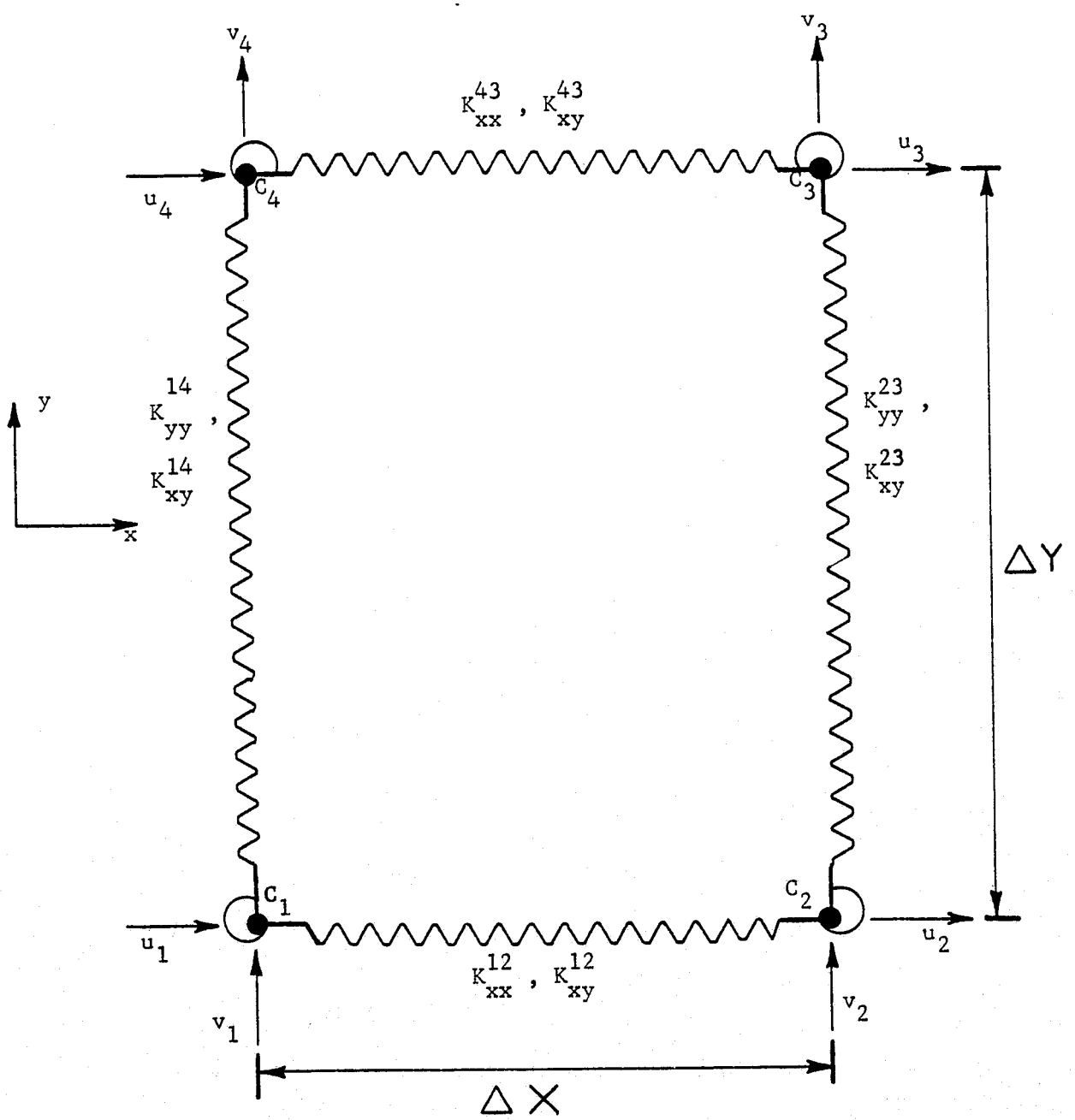

FIGURE 5. A TYPICAL LHR ELEMENT

$$U = \frac{1}{2} K_{xx}^{12} (u_2 - u_1)^2 + K_{xy}^{12} \left\{ \frac{v_4 - v_1}{2} + \frac{v_3 - v_2}{2} \right\} (u_2 - u_1)$$

$$+ \frac{1}{2} K_{xx}^{43} (u_3 - u_4)^2 + K_{xy}^{43} \left\{ \frac{v_4 - v_1}{2} + \frac{v_3 - v_2}{2} \right\} (u_3 - u_4)$$

$$+ \frac{1}{2} K_{yy}^{14} (v_4 - v_1)^2 + K_{xy}^{14} \left\{ \frac{u_3 - u_4}{2} + \frac{u_2 - u_1}{2} \right\} (v_4 - v_1)$$

$$+ \frac{1}{2} K_{yy}^{23} (v_3 - v_2)^2 + K_{xy}^{23} \left\{ \frac{u_3 - u_4}{2} + \frac{u_2 - u_1}{2} \right\} (v_3 - v_2)$$

$$+ \frac{1}{2} C_1 \left\{ \frac{(v_2 - v_1)}{\Delta x} + \frac{(u_4 - u_1)}{\Delta y} \right\}^2$$

$$+ \frac{1}{2} C_2 \left\{ \frac{(u_3 - u_2)}{\Delta y} + \frac{(v_2 - v_1)}{\Delta x} \right\}^2$$

$$+ \frac{1}{2} C_3 \left\{ \frac{(u_3 - u_2)}{\Delta y} + \frac{(v_3 - v_4)}{\Delta x} \right\}^2$$

$$+ \frac{1}{2} C_4 \left\{ \frac{(u_1 - u_4)}{\Delta y} + \frac{(v_4 - v_3)}{\Delta x} \right\}^2 \quad . \qquad (7)$$

It is desirable to determine an elemental stiffness matrix such that

$$\begin{bmatrix} & & \\ & K_e & \\ & & \end{bmatrix} \begin{bmatrix} u_1 \\ v_1 \\ \cdot \\ \cdot \\ \cdot \\ \cdot \\ u_4 \\ v_4 \end{bmatrix} = \begin{bmatrix} F_{x_1} \\ F_{y_1} \\ \cdot \\ \cdot \\ \cdot \\ F_{x_4} \\ F_{y_4} \end{bmatrix} \qquad (8)$$

This is accomplished by relating the node forces to the partial derivatives of the total strain energy. That is

$$F_{x_i} = \frac{\partial U}{\partial u_i}$$

and (9)

$$F_{y_i} = \frac{\partial U}{\partial v_i} \quad .$$

For example,

$$\frac{\partial U}{\partial u_1} = F_{x_1} = K_{xx}^{12}\left[u_1 - u_1\right] + K_{xy}^{12}\left[\frac{v_1}{2} - \frac{v_4}{2} + \frac{v_2}{2} - \frac{v_3}{2}\right]$$

$$+ \frac{1}{2} C_1 \left[2\left(\frac{v_1 - v_2}{\Delta x\, \Delta y}\right) + \frac{2(u_1 - u_4)}{(\Delta y)^2}\right]$$

$$+ \frac{1}{2} C_4 \left[\frac{2(v_4 - v_3)}{\Delta x\ \Delta y} + \frac{2(u_1 - u_4)}{(\Delta y)^2}\right] \quad . \qquad (10)$$

Expansion of this relation will give the elements in the first row of the matrix $[K_e]$. Subsequent derivatives taken with respect to the other degrees of freedom generate the remaining rows.

The spring constants used in the formulation must be related to the constituent's elastic properties. This is accomplished via the relations

$$K_{xy}^{ij} = Q_{12} \qquad \text{for } i,j = 1,\ldots 4$$

$$K_{xx}^{ij} = Q_{11}\frac{\Delta y}{\Delta x} \qquad \text{for } i,j = 1,\ldots,4$$

$$K_{yy}^{ij} = Q_{22}\frac{\Delta x}{\Delta y} \qquad \text{for all } i,j = 1,\ldots,4$$

$$C_i = \frac{1}{4} Q_{33}\, \Delta x\, \Delta y \text{ for all } i = 1,\ldots,4$$

where [Q] is defined as the constitutive stiffness matrix in the usual manner as

$$\begin{bmatrix} \sigma_x \\ \sigma_y \\ \tau_{xy} \end{bmatrix} = \begin{bmatrix} & Q & \end{bmatrix} \begin{bmatrix} \varepsilon_x \\ \varepsilon_y \\ \gamma_{xy} \end{bmatrix} . \tag{11}$$

Specifying these relations is tantamount to assuming that the material in each element is completely homogeneous. The desired heterogenity arises from the fact that the Q_{ij}'s are different for the fiber, matrix, and interface elements.

The Energy-Release Rate

The local rupture criterion used in this work is a generalized version of the ordinary energy-release rate (or crack-driving force) quantity of LEFM. In formulating it, attention must be placed on the complete structure. The discretized form of the equations of equilibrium for a complete structure can be represented by the matrix equation

$$\left[\underset{\sim}{k}\right] \underset{\sim}{u} = \underset{\sim}{F} \quad , \tag{12}$$

where $\underset{\sim}{k}$ is the structural stiffness matrix, $\underset{\sim}{u}$ is the nodal displacement vector and $\underset{\sim}{F}$ the applied nodal load vector. The energy-release rate G can be defined in a global sense by relating it to the change in work done by the applied loading and the strain energy during a virtual crack extension. This is

$$G \equiv \frac{dW}{da} - \frac{dU}{da} \tag{13}$$

where

$$W \equiv \underset{\sim}{u}^T \underset{\sim}{F} \tag{14}$$

is the work done by the applied loading,

$$U \equiv \frac{1}{2} \underset{\sim}{u}^T [\underset{\sim}{k}] \underset{\sim}{u} \tag{15}$$

is the strain energy and a represents the crack length. (In these equations, the superscript T denotes the transpose.)

When Equations (14) and (15) are introduced into Equation (13), it is found that

$$G = \frac{d\underset{\sim}{u}^T}{da} \underset{\sim}{F} - [\underset{\sim}{k}] \underset{\sim}{u} + \underset{\sim}{u}^T \frac{d\underset{\sim}{F}}{da} - \frac{1}{2} \underset{\sim}{u}^T \frac{d}{da} [\underset{\sim}{k}] \underset{\sim}{u} \quad . \tag{16}$$

It can be seen from Equation (12) that the quantity within the braces of Equation (16) is a null vector. Furthermore, if $\underset{\sim}{F}$ is independent of the crack length, then the second term also vanishes. Equation (16) therefore reduces to

$$G = - \frac{1}{2} \underset{\sim}{u}^T \frac{d}{da} [\underset{\sim}{k}] \underset{\sim}{u} \quad . \tag{17}$$

Now, it can be considered that the only contribution to the matrix $\frac{d}{da} [\underset{\sim}{k}]$ is that due to the stiffness matrix K of the element containing the crack tip. If $\underset{\sim}{u}$ denotes the displacement vector of the nodes of the element only, then Equation (17) can be used to obtain an approximation of G that can be written as

$$G = \frac{\underset{\sim}{u}^T [K_b] \underset{\sim}{u} - u^T [K_a] \underset{\sim}{u}}{2\Delta a} \tag{18}$$

where $[K_b]$ ($[K_a]$) is the elemental stiffness matrix before (after) an extension Δa of the crack within the element. Recognizing that

$$U_e = \frac{1}{2} \underset{\sim}{u}^T [K] \underset{\sim}{u} \tag{19}$$

is the elemental strain energy, then an alternative form of Equation (18) is

$$G = \frac{U_{e_b} - U_{e_a}}{\Delta a} \quad . \tag{20}$$

A similar development for the energy-release rate occurs in the recently published papers by Hellen, et al. [6,7].

Program Solution Techniques

To use the analysis that has been developed thus far, the material properties of the constituents and the micromechanical geometry must be specified. (The material properties are also used to determine the homogeneous orthotropic properties of the bulk composite through an effective modulus or volume fraction technique.) The way in which the constituent properties and the geometry are used to generate elemental stiffnesses for assemblage into the LHR will be described next.

There are two classes of nodal points used in the LHR. The first consists of the points on the boundary of the LHR where displacements are prescribed. The nodal points in the interior of the LHR having unknown displacements make up the second class. It is useful to assemble the stiffness matrix in such a way that these two groups are isolated. The partition used here is

$$\begin{bmatrix} [k_{22}] & [k_{23}] \\ [k_{32}] & [k_{33}] \end{bmatrix} \begin{Bmatrix} \{u_2\} \\ \{u_3\} \end{Bmatrix} = \begin{Bmatrix} \{F_2\} \\ \{F_3\} \end{Bmatrix} \quad . \tag{21}$$

In Equation (21), the subscripts do not refer to nodes, but to the nodal point classification just described. That is (u_2) represents the prescribed displacement vector of the peripheral points while (u_3) is the vector of the unknown displacements for which a solution is desired. Note that the number 1 was not used as a subscript because it is more convenient to reserve it for specified zero displacements.

By performing the matrix multiplication indicated in Equation (21), the following two equations are obtained:

$$[k_{22}] \{u_2\} + [k_{23}] \{u_3\} = \{F_2\} \tag{22}$$

$$[k_{32}] \{u_2\} + [k_{33}] \{u_3\} = \{F_3\} = \{0\} \quad . \tag{23}$$

Most often, it is either impossible or inefficient to store large matrices such as $[k_{33}]$ in the computer's central processor core area. For this reason $[k_{33}]$ is stored externally. The external storage can be minimized by utilizing the fact that the $[k_{33}]$ matrix is always symmetric and banded; the latter term indicating the tendency for nonzero values to cluster around the diagonal of the matrix. By taking advantage of matrix partitioning (i.e., the grouping of prescribed and unprescribed degrees of freedom), symmetry, and the banded nature of the stiffness matrix, storage of only a small portion of the original total stiffness matrix is required. However, this reduced storage requirement can still be very large in some problems.

Solution of Equation (23) is accomplished through the use of Gaussian elimination with back substitution. Small parts of stored $[k_{33}]$ matrix are brought into core as required in this operation. Assemblage of the required parts of the stiffness matrix is done by the direct stiffness method.* Components that would ordinarily fall within the $[k_{22}]$ and $[k_{23}]$ submatrices are discarded. Stiffness components that fall within the $[k_{32}]$ submatrix are used in a nonzero $\{F_3\}$ vector. Finally, those values of $[k_{33}]$ falling on or above its diagonal are stored externally.

Once the boundary conditions have been prescribed, an out-of-core type solution of the partitioned LHR stiffness matrix with boundary conditions for a unit load is performed. The resulting displacement vector is then used to calculate the potential fracture energies associated with each of the four fracture codes. Ratios of the prescribed critical energy levels to these calculated energies are next computed. The applied load is then adjusted such that the highest ratio becomes exactly equal to unity. This critical region (if one exists) is allowed to break in one of the four ways (codes) described above. Appropriate modifications are then made to the LHR stiffness matrix.

* A detailed description of the direct stiffness assemblage technique used in this work is given by Desai and Abel [8].

Because the system is completely linear elastic, a solution for another load level can then be performed in exactly the same manner. In this way, the properties of a crack tip damage zone as a function of an increasing applied load can be generated.

As each local rupture occurs, the prescribed boundary conditions must be adjusted. If the crack has propagated in a self-similar fashion, this is readily done by shifting the origin (cf, Figure 2). If not, this may present some very real difficulties for then the continuum solution no longer exactly applies and some approximations must be used for setting the boundary conditions. The larger the LHR, the less likely this will be necessary. Of course, large LHR's require large solution times even though storage is generally not a problem because of the out-of-core solution. It is likely that the boundary condition problem can be handled by introducing a flexible boundary-condition scheme (see Recommended Future Research section), or, possibly, by allowing the fractured LHR to interact in a hybrid continuum model for future boundary updating.

Verification of Computational Model

Before performing extensive calculations on composite materials, it is appropriate to verify the computational model by checking it against known solutions. By letting the model represent a linear elastic homogeneous material, two checks can be made. These are on the displacements in the LHR and on the calculated energy-release rate.

Consider the element configuration shown in Figure 1. A check on the calculated displacements can be made by imposing the continuum derived boundary conditions on a LHR region where the LHR is used to simulate a completely homogeneous region. Displacements at the node points were calculated and used to calculate average stresses within the elements. The computed values of stress and displacement were then compared with values calculated by the continuum solution for the interior of the region. Agreement between the two solutions was found to be quite good. The check thus provided one necessary verification of both the LHR element itself and of the finite element assemblage and solution procedure as well.

As described in the above, all of the energy released within the element at the crack tip, if an incremental amount of crack extension were to occur, should equal the strain energy-release rate, G. To check this, cal-

culations were made using the exact near crack tip displacement field for an elastic isotropic material. The energy-release rate obtained from this calculation is denoted by G^* to distinguish it from the exact theoretical value G. The necessity for introducing this distinction is as follows.

The quantity G can be formally defined in terms of a virtual crack extension as the total change in energy of the body per unit area of crack extension; cf, Equation (13). The quantity G^*, on the other hand, reflects only the change in energy of the element near the crack tip. Consequently, G^* does not include the change in energy of the remainder of the body as the crack extends. In order to account for the contribution arising from the change in energy of the remainder of the structure, a term denoted by δG^* was formulated. The sum $G^* + \delta G^*$ is then taken as the appropriate approximation to G in this work.

A numerical experiment was performed to calculate G^* and δG^* as a function of the aspect ratio $\Delta y/\Delta x$ of the LHR elements. The results are shown in Table II. It is quite evident that the sum $G^* + \delta G^*$ provides an accurate approximation to G for the elongated aspect ratios that are convenient to use in the calculations on fiber composite materials.

There are two further points of interest about the results shown in Table II. First, while it may be surprising that δG^* and G^* are functions only of the ratio of Δy to Δx, this is a direct consequence of the use of rigid boundary conditions which put the near tip displacements into the energy relationship used to calculate G. The resulting expression contains only the aspect ratio, $\Delta y/\Delta x$. Second, while it might be expected that δG^* should converge to zero as the grid spacing is collapsed (i.e., as both $\Delta y \to 0$ and $\Delta x \to 0$), it can be seen that this was not the case. Instead, convergence is obtained only as the ratio of Δy to Δx becomes large. Then, δG^* approaches a value equal to 11 percent of G while G^* converges to value equal to 86 percent of G.

A number of different computations for heterogeneous materials have also been made. These runs have been made with a model similar to the one shown in Figure 3. Preliminary results indicate that most of the initially envisioned modes of failure are exhibited by the model. A discussion of these results is given in the next section of this report.

TABLE II. AN EXAMPLE CALCULATION OF THE STRAIN ENERGY RELEASE RATE AS A FUNCTION OF THE GRID SIZE RATIO FOR A HOMOGENEOUS LINEAR ELASTIC MATERIAL

$\frac{\Delta y}{\Delta x}$	$\frac{G^*}{G}$	$\frac{\delta G^*}{G}$	$\frac{(G^* + \delta G^*)}{G}$
1	0.71	0.75	1.46
2	0.72	0.42	1.14
4	0.77	0.25	1.02
8	0.81	0.18	0.99
16	0.83	0.15	0.98
32	0.84	0.13	0.97
64	0.85	0.12	0.97
128	0.86	0.11	0.97
256	0.86	0.11	0.97

EXAMPLE COMPUTATIONAL RESULTS FOR FRACTURE OF FIBER-REINFORCED COMPOSITES

A number of computations have been performed using the analysis technique described in the preceding section of this report. As discussed in this section, the results demonstrate the ability of the model to exhibit most of the actual failure mechanisms in fiber-reinforced composite materials. These include fiber-matrix debonding, fiber bridging, matrix bridging, and matrix crazing. The only important micromechanical mechanism that the model currently does not explicitly represent is fiber pull-out.*

Calculations With Arbitrarily Varied Rupture Properties

The following describes a series of example calculations in which the various fracture mechanisms are made to manifest themselves. The results shown here were obtained by varying each of the constituent's rupture properties and, in some instances, the constituent elastic properties, over a wide range of values. Hence, the actual values selected to perform these example computations are not totally realistic. The intent here is to provide a qualitative verification that the model is capable of achieving its primary function rather than to make realistic predictions.

Unless otherwise stated, the elastic constants used in the calculations are those given in Table III.

TABLE III. ELASTIC PROPERTIES USED IN THE SIMULATION OF A GRAPHITE EPOXY COMPOSITE

Constituent	E Elastic Modulus (ksi)	ν Poisson's Ratio
Fiber	28,000	0.3
Matrix	495	0.3
Interface	495	0.3

* As discussed in the Recommended Future Research section of this report, steps to incorporate both fiber pull-out and interply delamination can be performed in a straightforward manner in subsequent work.

These properties were intended to be nominally equivalent to those of a graphite epoxy composite with a volume fraction of fiber equal to 70 percent. Consistent with these values are the following properties of the bulk composites:

$$E_1 = 18{,}000 \text{ ksi}, \quad \nu_{12} = 0.25$$

$$E_2 = 690 \text{ ksi}, \quad G = 3{,}000{,}000.$$

Note that the constituents were assumed to be isotropic. However, the model does not require this.

The first computation to be discussed is shown in Figure 6. This result illustrates the fiber-matrix debonding mechanism, a mechanism that occurs in a large number of cases. Typically, a crack will advance through the matrix and then vertically separate or axially split the interface. In this example, the interfacial elements were made relatively weak while the fiber and matrix material were given relatively average strengths. The loading in this example was purely Mode I.* It was found that axial splitting is even more prevalent when Mode II loads are applied.

Matrix crazing typically occurs when a crack advancing through the matrix reaches a very strong stiff fiber. Figures 7 and 8 show typical examples. If the fiber does not break, a number of local events occur in the matrix that seem to approximate matrix crazing. Typically, the crazing does not occur on the uncracked side of the fiber. The reason is that the displacements on the cracked side of the fiber are "locked in" by the adjacent highly stretched fiber. Consequently, crazing usually occurs when strong very stiff fiber properties are inserted into the model together with average strength and stiffness properties for the matrix and interface.

Matrix bridging is shown in Figure 9. This phenomenon typically occurs when the fibers are considered to be stiff, but weak. In these instances the matrix and interface are capable of withstanding higher elongation than the fiber. So, they will remain intact while the fiber cracks. In the example shown in Figure 9, some additional interfacial response can also be noticed.

---

* Unless otherwise stated, in the calculations described in this section of the report, the applied loading was a tensile normal stress in the direction parallel to the fibers.

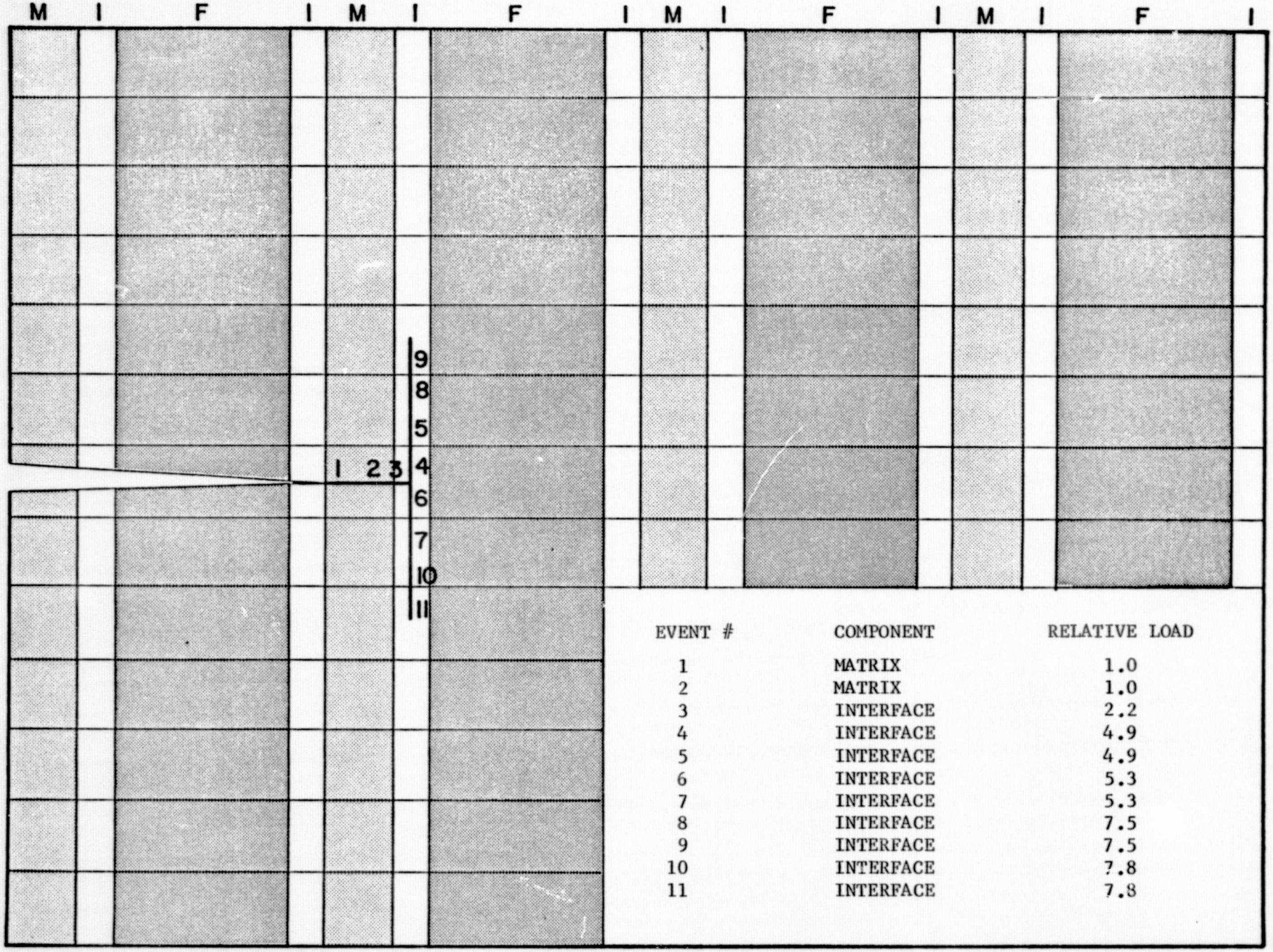

EVENT #	COMPONENT	RELATIVE LOAD
1	MATRIX	1.0
2	MATRIX	1.0
3	INTERFACE	2.2
4	INTERFACE	4.9
5	INTERFACE	4.9
6	INTERFACE	5.3
7	INTERFACE	5.3
8	INTERFACE	7.5
9	INTERFACE	7.5
10	INTERFACE	7.8
11	INTERFACE	7.8

FIGURE 6. EXAMPLE CALCULATION WITH WEAK INTERFACE SHOWING MATRIX-FIBER DEBONDING

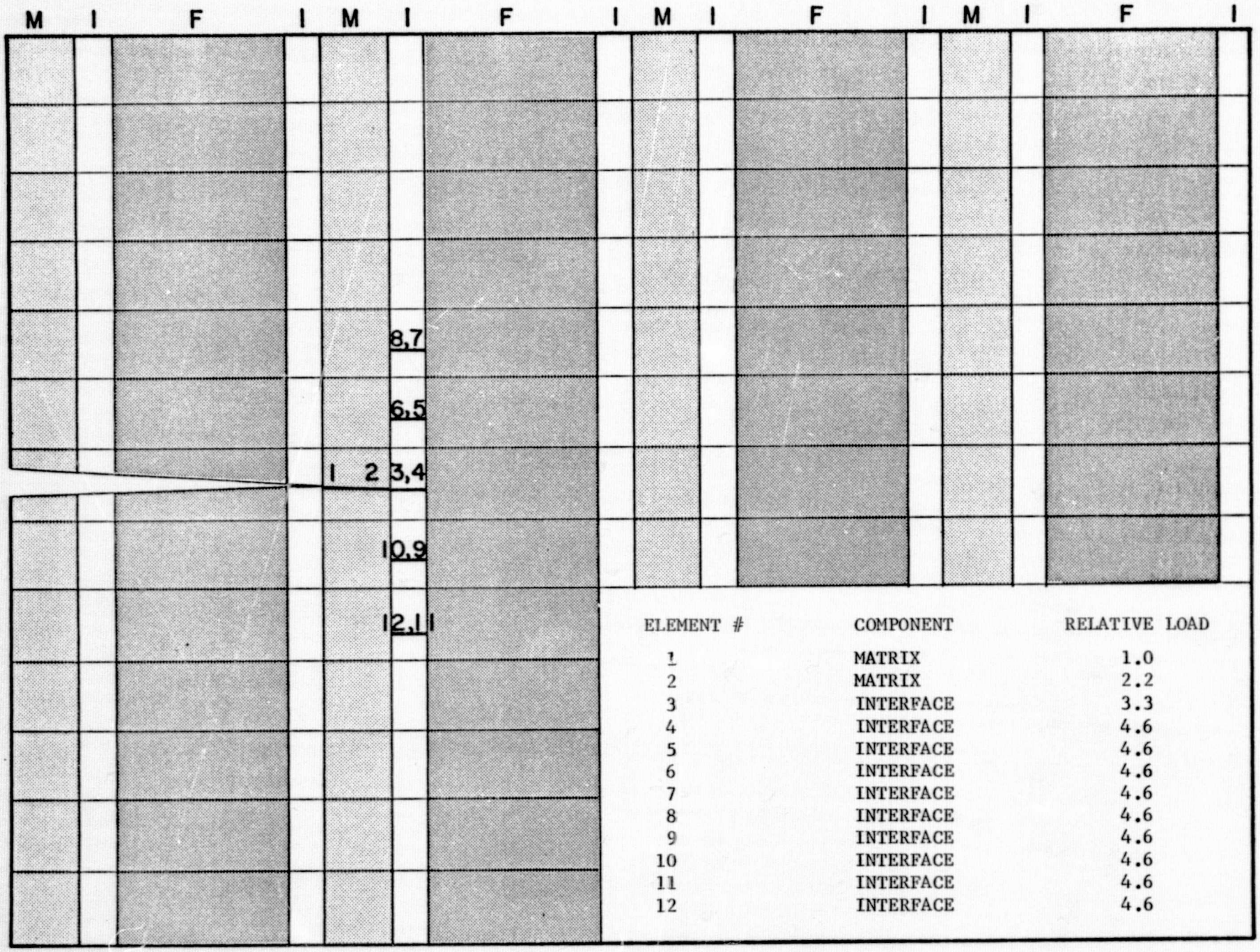

ELEMENT #	COMPONENT	RELATIVE LOAD
1	MATRIX	1.0
2	MATRIX	2.2
3	INTERFACE	3.3
4	INTERFACE	4.6
5	INTERFACE	4.6
6	INTERFACE	4.6
7	INTERFACE	4.6
8	INTERFACE	4.6
9	INTERFACE	4.6
10	INTERFACE	4.6
11	INTERFACE	4.6
12	INTERFACE	4.6

FIGURE 7. EXAMPLE CALCULATION WITH STRONG STIFF FIBERS AND WEAK INTERFACE SHOWING MATRIX CRAZING

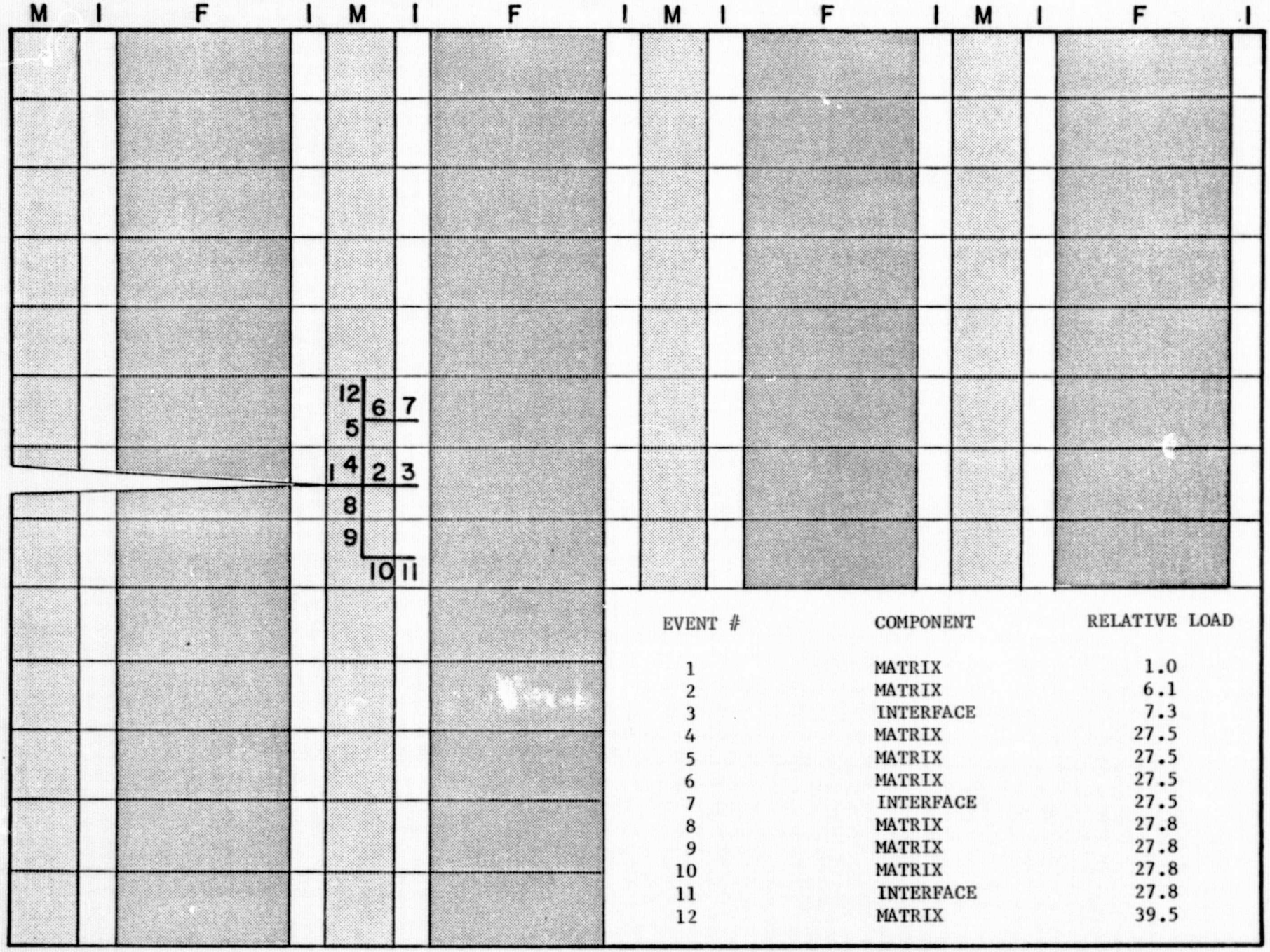

EVENT #	COMPONENT	RELATIVE LOAD
1	MATRIX	1.0
2	MATRIX	6.1
3	INTERFACE	7.3
4	MATRIX	27.5
5	MATRIX	27.5
6	MATRIX	27.5
7	INTERFACE	27.5
8	MATRIX	27.8
9	MATRIX	27.8
10	MATRIX	27.8
11	INTERFACE	27.8
12	MATRIX	39.5

FIGURE 8. EXAMPLE CALCULATION WITH STRONG STIFF FIBERS SHOWING MATRIX CRAZING

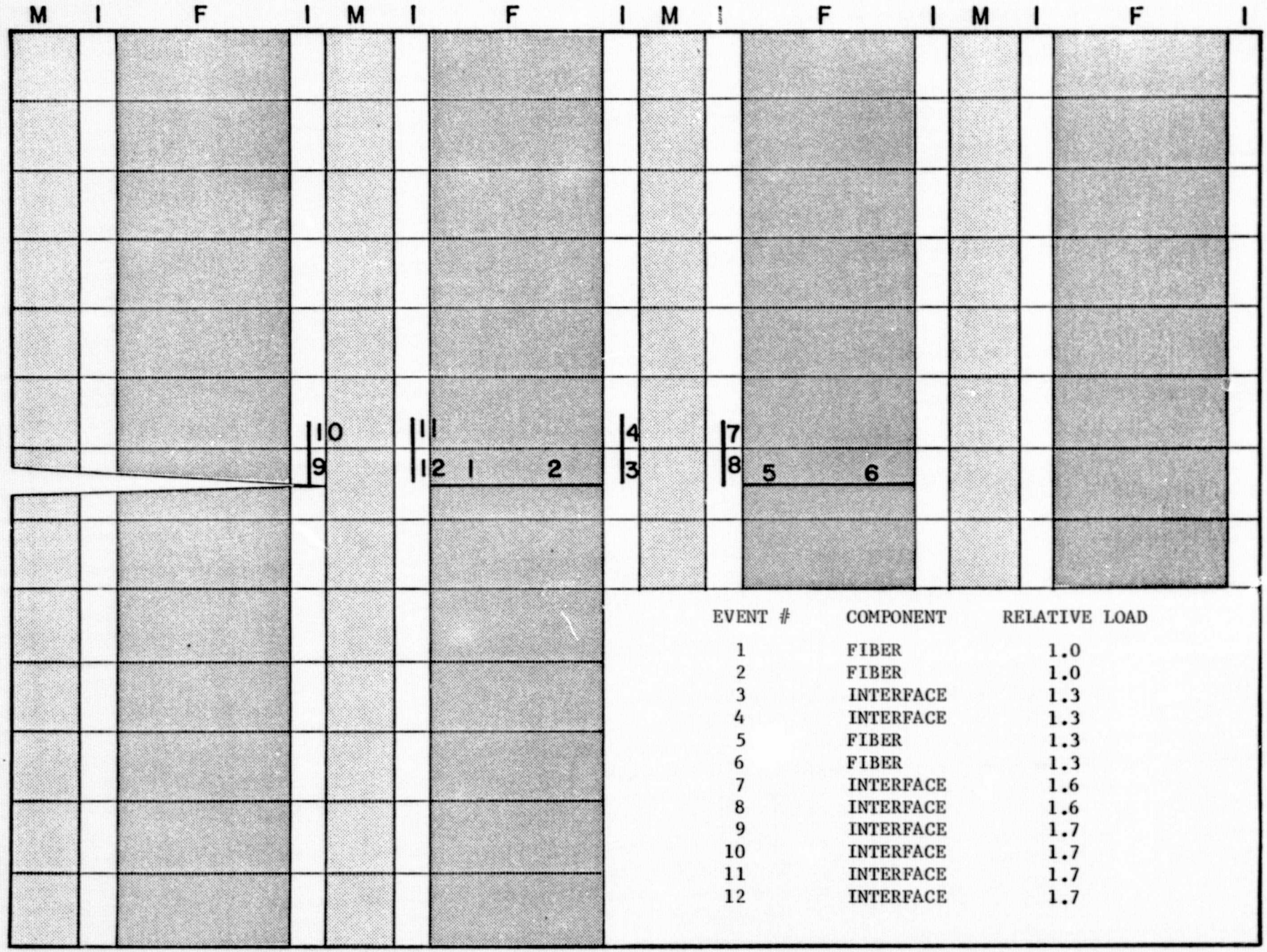

EVENT #	COMPONENT	RELATIVE LOAD
1	FIBER	1.0
2	FIBER	1.0
3	INTERFACE	1.3
4	INTERFACE	1.3
5	FIBER	1.3
6	FIBER	1.3
7	INTERFACE	1.6
8	INTERFACE	1.6
9	INTERFACE	1.7
10	INTERFACE	1.7
11	INTERFACE	1.7
12	INTERFACE	1.7

FIGURE 9. EXAMPLE CALCULATION WITH STIFF WEAK FIBERS SHOWING MATRIX BRIDGING

Fiber bridging is more prevalent when the fiber modulus does not greatly exceed the matrix modulus. (In graphite epoxy, the modulus ratio is on the order of 50 and fiber bridging does not then seem to occur.) Figure 10 demonstrates this behavior. Fiber bridging can also be related to the microstructural geometry. That is, in computations performed with relatively thin fibers, this mechanism becomes more dominate.

It should be emphasized that the examples given in the above deliberately used exactly the same LHR configuration and applied loading. The program has the flexibility to consider different loading conditions and LHR geometries. However, this option was not exercised here because of the complications that would be added to the interpretation of the results. That is, it would be difficult to separate the effects due to the LHR geometry and loading from those due to variations in the rupture strength and modulus. Such calculations will be deferred until further refinements have been incorporated into the model. Again, the purpose of the computations given in Figures 6-10 is to give a qualitative demonstration that the model is capable of coping with the micromechanical failure processes involved in the fracture of composite materials, not to produce precise quantitative results.

Finally, note that the relative load levels at which each individual fracture event occurs is recorded. (These levels are relative to the load level at which the initial rupture event occurs.) It can be seen that the load level must ordinarily be increased to obtain additional rupture events, or, in other words, in order to enlarge and propagate the crack-tip damage zone. This can be contrasted with the behavior of completely homogeneous, perfectly brittle materials represented by LEFM where crack extension, once initiated, would continue in a catastrophic manner under a constant load level. The initial stages of the fracture event in fiber composite materials therefore can obviously be characterized in terms of a stable growth process. This suggests that a modification of the crack growth resistance curve (R curve) approach developed for the fracture of ductile materials could be useful for studying fractures in fiber composite materials. Such an approach, it might be mentioned, has already been suggested in the literature; for example, by Gaggar and Broutman [9]. However, these approaches are usually semiempirical in nature, relying heavily on LEFM concepts. The present approach, in contrast, should be able to make a direct prediction of the crack growth resistance parameter purely from fundamental-level considerations.

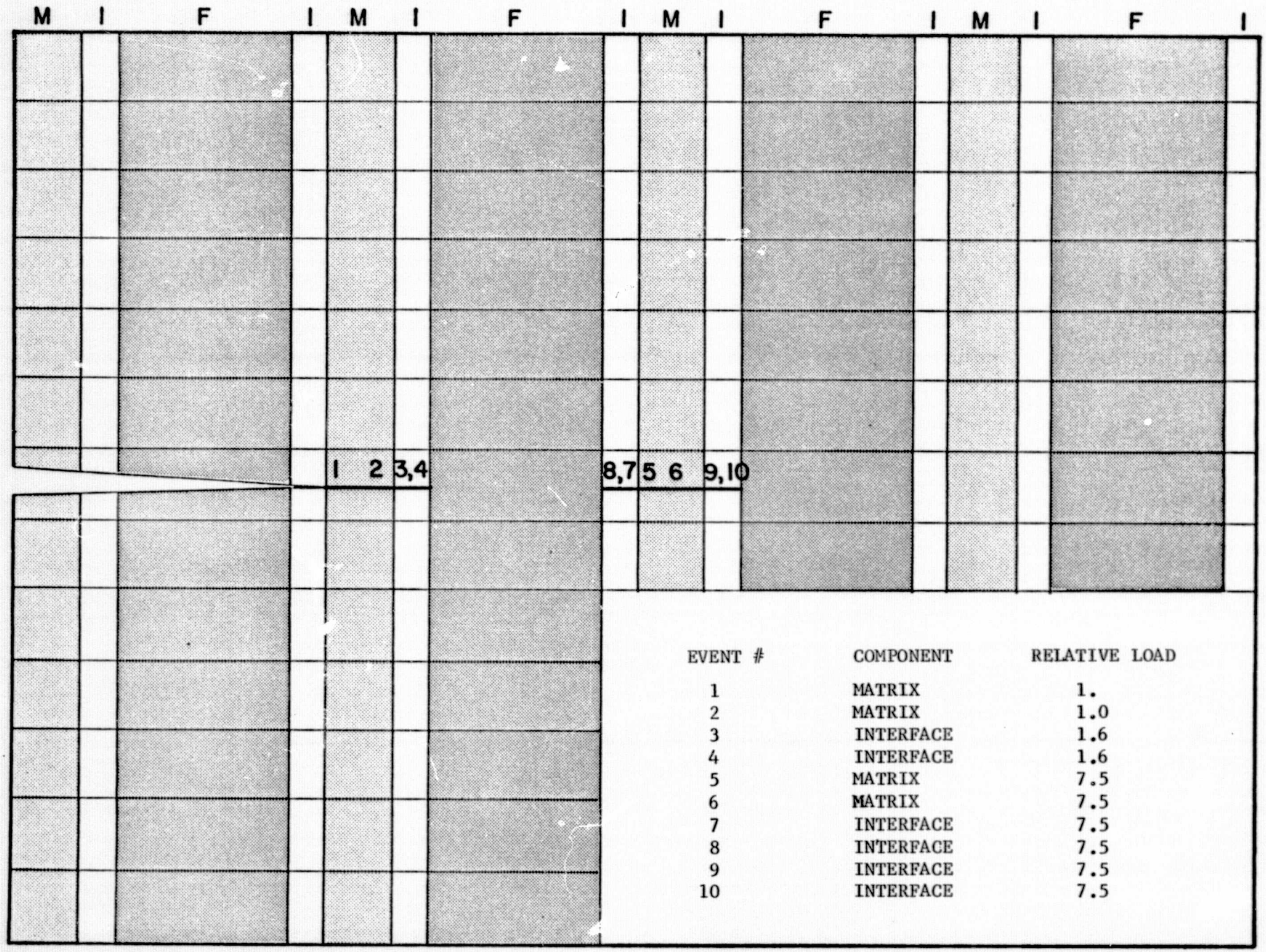

FIGURE 10. EXAMPLE CALCULATION WITH STIFF MATRIX SHOWING FIBER BRIDGING

Comparison of Calculated Results with VPISU Experimental Data

The computations described in the preceding section demonstrate that the model developed in this report displays the various micromechanical failure mechanisms actually exhibited by fiber reinforced composites. A more quantitative verification is also possible. This can be done by comparing the predictions of the model with the experimental results obtained in the concurrent NASA-Ames sponsored research at Virginia Polytechnic Institute and State University (VPISU) by Brinson and Yeow [10]. They have measured the strengths of both unidirectional and angle ply graphite/epoxy composites using unnotched, single edge notched, and double edge notched specimens with the crack introduced at various angles to the fiber direction. In this section, the model will be used to estimate the strengths of some of the Brinson-Yeow unidirectional notched tests using input values inferred from their unnotched tests.

A precise prediction of failure loads is not to be expected at the present stage of this research for several reasons. First, because of the stable damage growth that precedes fracture in composites, computations performed using rigid boundary conditions (which artifically constrain the damage growth process) will not be realistic. The predictions of the initial local failure event--the threshold of stable damage growth--should be reasonably well predicted, however. This load level will therefore be taken as the prediction of the model to be compared with the experimental measurements. It should be recognized that, because of the neglect of the stable growth regime, these should underestimate the actual failure loads.

A second reason for the lack of precision inherent in the present predictive capability is that the constituent properties needed in the model have not been properly determined as yet. As in the preceding section, linear elastic-perfectly brittle behavior can be assumed with handbook values being taken for the elastic properties. Rupture properties are not as readily available, however. To circumvent this difficulty, the experimental results on unnotched specimens obtained by Brinson and Yeow can be used. Their data on the strengths of unnotched coupons pulled to failure with the load in the fiber direction ($\theta = 0°$) and normal to the fiber direction ($\theta = 90°$) are given in Table IV. Relying on their observation that matrix failure occurred in

TABLE IV. CRITICAL VALUES FOR MATRIX FAILURE IN GRAPHITE EPOXY COMPOSITES

Angle Between Load and Fiber Directions	Experimental Values[a]			Critical Strain Energy Density (in. lb/in.^{3})
	Elastic Modulus (ksi)	Fracture Stress (ksi)	Fracture Strain (%)	
0°	18,200	154.7	0.82	576
90°	1,700	6.1	0.44	13.6

(a) Data of Brinson and Yeow [10] on unidirectional unnotched specimens for a loading rate of 2×10^{-3} inches/min.

virtually all cases, the critical strain energy density quantity can be calculated (i.e., $\frac{1}{2}E\varepsilon^2$) for use in the model. These figures are given in the last column in Table IV.

As discussed on page 11 of this report, the applied loads acting on the body are communicated to the crack tip elements via the anisotropic elastic stress intensity factors. For test specimens, such as the single and double edge notched configurations used by Brinson and Yeow, there is a term in the stress intensity factor that contains the effects of the finite geometry. This term is not the same for anisotropic and isotropic bodies. However, in view of the approximate nature of the present calculations, the refinement added through the use of the rather complicated anisotropic expression was not believed to be warranted. Hence, the isotropic expressions were used. For Mode I loading, these have the form.

$$K_I = \sigma a^{\frac{1}{2}} Y \tag{24}$$

where σ is the applied stress normal to the crack plane, a is the crack length and Y is a dimensionless function of the specimen geometry. For the double edge notched configuration

$$Y = 1.99 + 0.76\left(\frac{a}{W}\right) - 8.48\left(\frac{a}{W}\right)^2 + 27.36\left(\frac{a}{W}\right)^2 , \tag{25}$$

while for the single edge notched configuration

$$Y = 1.99 - 0.41\left(\frac{a}{W}\right) + 18.7\left(\frac{a}{W}\right)^2 - 38.48\left(\frac{a}{W}\right)^3 + 53.85\left(\frac{a}{W}\right)^4 , \tag{26}$$

where W is the plate width.

For a given crack length and load-fiber orientation in either the single or double edge notched configuration, the load corresponding to the threshold of damage is determined by a single calculation. This is due to the linear elastic material behavior assumed in the current model. That is, a computation can be performed for an estimated value of K_I. The solution can then be scanned to determine the highest strain energy density in any matrix element. By "scaling up" the solution to force this value to match

the critical value given in Table IV, the value of K_I corresponding to the threshold of damage is determined. The final step is to use Equation (24) to calculate the applied stress for direct comparison with the experimental results.

Comparisons of the calculated results as a function of crack length with the Brinson-Yeow results on unidirectional composites are shown in Figures 11 and 12 for the single and double edge notch configurations, respectively. Note that a semilog format is used (so that both the 0° and the 90° fiber-load angle results can be shown on the same plot) and this may make the agreement appear to be better than it really is. Nevertheless, in view of the remarks made in the preceding section, the prediction is reasonably accurate and, as expected, generally provides a lower bound to the experimental data. Note also that the unnotched result ($\frac{a}{W} = 0$) is included on the theoretical curve to emphasize that this point was used to construct the curve.

Finally, comparisons with experimental data can also be made for the case of cracks introduced at an angle to the fiber direction. An example computation is shown in Figure 13. The threshold-of-damage load level calculations are made as above except that both the Mode I and Mode II stress intensity factors now are involved in the computation. These have been taken as

$$K_I = \sigma a^{\frac{1}{2}} Y \sin^2 \phi$$

and

$$K_{II} = \sigma a^{\frac{1}{2}} Y \cos \phi \sin \phi \quad , \tag{27}$$

where ϕ is the angle between the crack plane and the fiber direction. A comparison between the predicted results and the Brinson-Yeow experimental results as a function of ϕ for a 0° load-fiber angle is shown in Figure 14. Again, it can be seen that the model provides a reasonable lower bound to the experimental results.

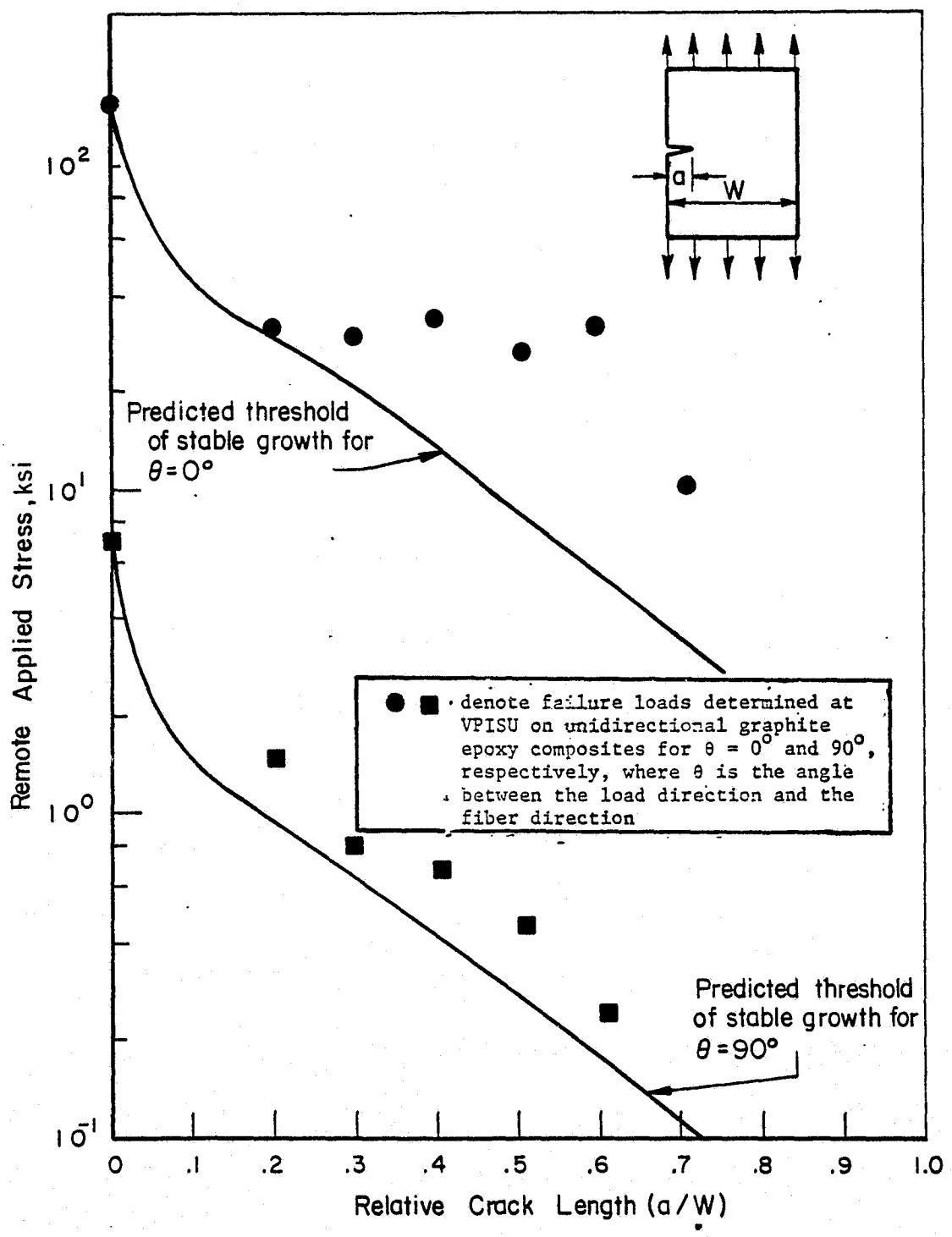

FIGURE 11. COMPARISON OF PREDICTED STABLE GROWTH THRESHOLD WITH EXPERIMENTAL FAILURE LOADS FOR SINGLE EDGE NOTCH SPECIMENS

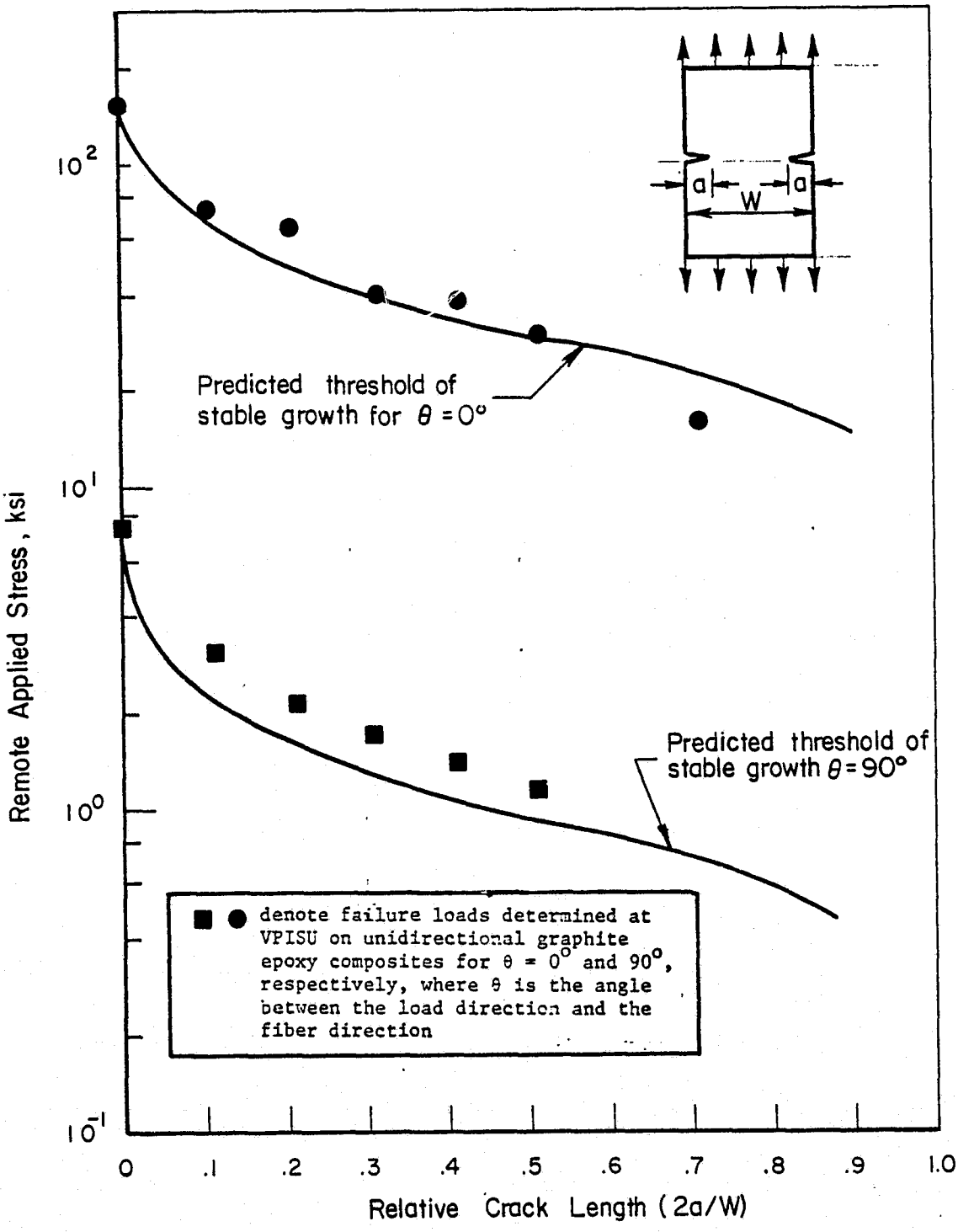

FIGURE 12. COMPARISON OF PREDICTED STABLE GROWTH THRESHOLD WITH EXPERIMENTAL FAILURE LOADS FOR DOUBLE EDGE NOTCH SPECIMENS

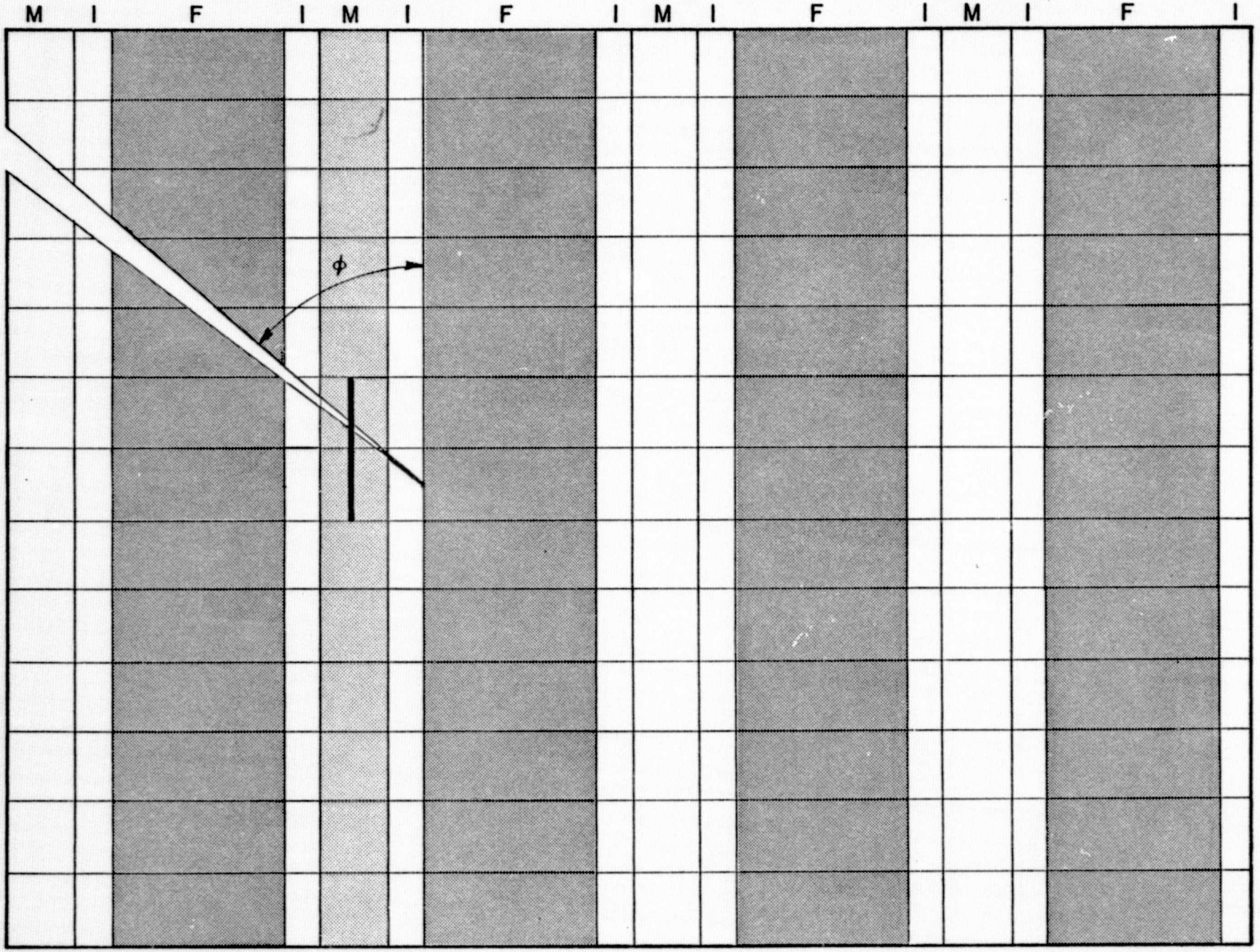

FIGURE 13. EXAMPLE CALCULATION FOR A FIBER COMPOSITE WITH AN ANGLE CRACK

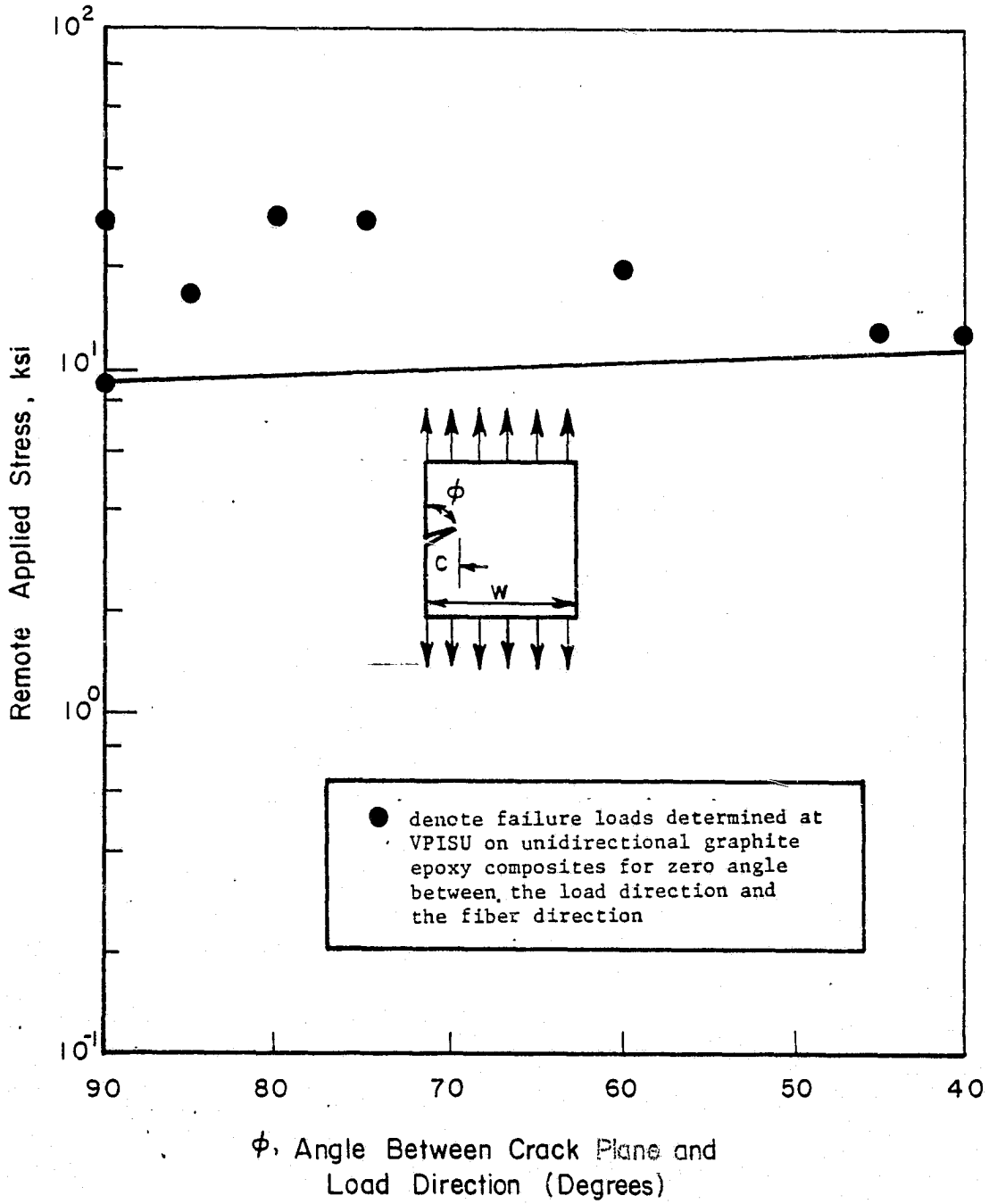

FIGURE 14. COMPARISON OF PREDICTED STABLE GROWTH THRESHOLD WITH EXPERIMENTAL FAILURE LOADS FOR SINGLE EDGE NOTCH SPECIMENS WITH ANGLE CRACKS

RECOMMENDED FURTHER RESEARCH

Being two dimensional, the model described in this report is so far limited in application to unidirectional laminates and can only reflect the local damage modes that occur in plane deformation. In subsequent work, it would be desirable to extend the model from two dimensions to three dimensions to treat angle ply laminates. In addition to treating the effect of different layups, new modes of damage (e.g., interply delamination, fiber pull-out) should also be included.

A straighforward extension of the model could be made by devising a three-dimensional LHR. But, the number of storage locations required for the three-dimensional grid would likely exceed the fast access storage of most computers. To circumvent this situation, the present two-dimensional model could be extended to angle ply laminates by considering laminates with an LHR only in a single ply. Figure 15 shows this concept. In the simplest case, the LHR can be confined to the most critical ply as the load level is increased. In general, there can be an LHR in each ply with attention shifted from one ply to another in turn. In either case, it would be necessary to assume that the interply interactions are not affected by the precise details of the local damage occurring in each ply.

In Figure 15a, a laminate containing a flaw is shown with generalized loading conditions. In this the first level of modeling, all of the plys are considered as homogeneous orthotropic layers. Displacements can be calculated in this model for any load level and applied to the boundaries of the local homogeneous region in each ply. Then, just as in the two-dimensional model, the LHR shown in Figure 15b can be monitored to determine the local rupture events and the extent of the damage zone at that load level. When significant crack growth has occurred in one or more plys, the first level model must, of course, be made to reflect this. But, the basic approach would not be changed thereby.

Two distinct techniques must be developed in order to obtain an accurate set of boundary displacements for each LHR when extensive damage occurs in that or in neighboring plys. The first is to incorporate the effect of the stiffness change in the LHR into the first level model of the laminate. The loading conditions would then be obtained from this modified first level model (i.e., one with locally reduced stiffnesses) to give the new boundary

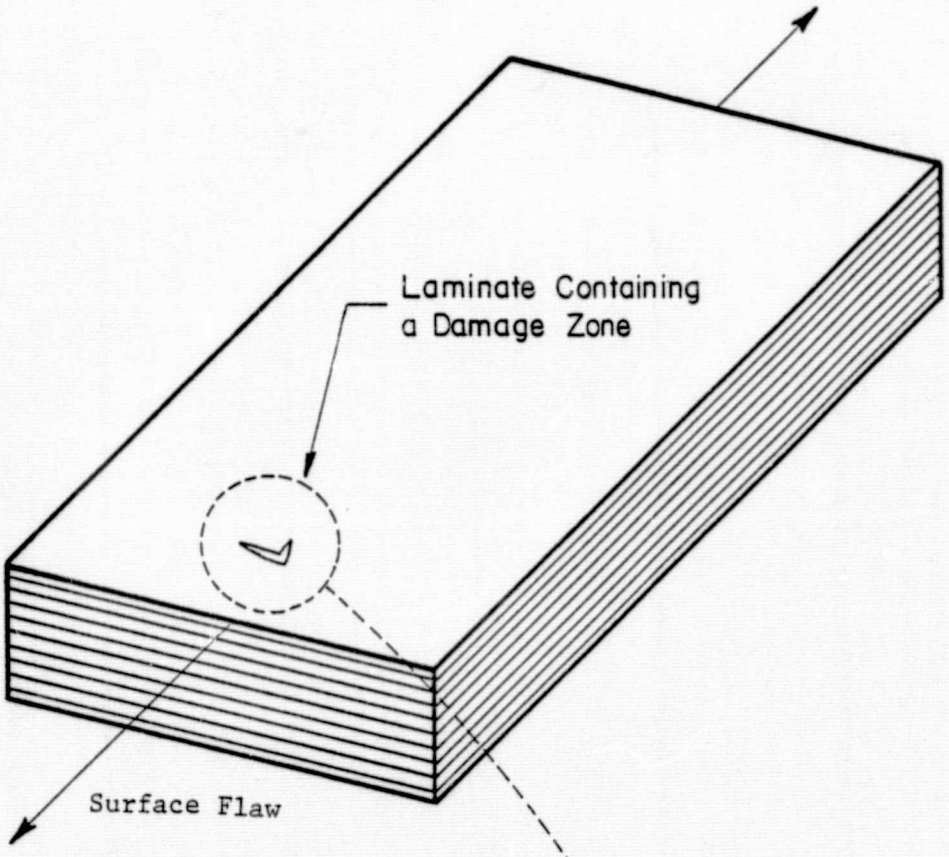

(a) First level of modeling.

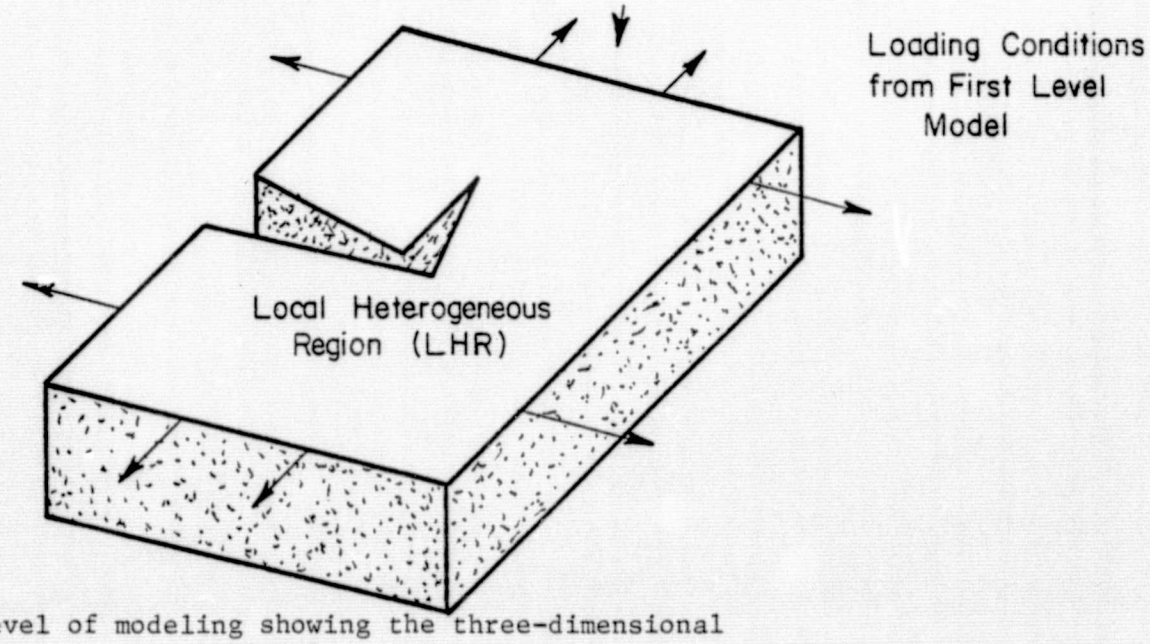

(b) Second level of modeling showing the three-dimensional representation of a single ply.

FIGURE 15. THREE-DIMENSIONAL MODEL FOR A LAMINATED PLATE

conditions for the LHR. In the second technique, the influence of the stiffness of the laminate away from the crack tip will be directly transferred to the LHR through what can be called a "flexible boundary condition" technique. This approach can be likened to placing a series of springs on the LHR boundary with stiffnesses taken from the first level model. The actual technique is more sophisticated than this, however, as follows.

In the work described so far, the peripheral elements in the LHR have been positioned according to the displacement field given by a completely linear elastic continuum solution for the given crack tip location and applied loads. This is not strictly correct even when the displacements are periodically updated as the crack extends in the LHR. Even in the absence of local damage, the highly nonlinear inhomogeneous nature of the crack-tip region in a composite will cause significant departures from the continuum displacements. A scheme for estimating these displacements based on a determination of the equilibrium state between the LHR and the continuum can be obtained by adapting the technique reported in Reference 3. Such a scheme has been referred to as the "flexible boundary condition" approach. The approach used so far can be called the "rigid boundary condition" approach because, even with periodic updating to reflect the progress of the crack through the LHR, the LHR does not directly affect the continuum region surrounding it. The flexible boundary condition approach, in contrast, accounts for the interaction.

Finally, the range of modes of damage should be extended over those of the two-dimensional model to include interply delamination and a "free-edge" effect. The general approach could be similar to that described in References 10 and 11. Attention should first be focused on through-the-thickness cracks in laminated plates under tension with part-through flaws being considered later. Of most importance, the three-dimensional model of an angle ply laminate should permit arbitrarily varied multidirectional layups to be explicitly considered. The properties for the ply moduli could be obtained from laboratory investigations, e.g., in the program being conducted for NASA-Ames at Virginia Polytechnic Institute and State University.

REFERENCES

[1] Mandell, J. F., Wang, S. S., and McGarry, F. J., "The Extension of Crack Tip Damage Zones in Fiber Reinforced Plastic Laminates", J. Composite Mat. 9 (1975) 266.

[2] Sih, G. C. and Liebowitz, H., "Mathematical Theories of Brittle Fracture", Fracture, Vol II, H. Liebovitz, Editor, Academic Press, New York, (1968) p 67.

[3] Gehlen, P. C., Hirth, J. P., Hoagland, R. G., and Kanninen, M. F., "A New Representation of the Strain Field Associated with the Cube-Edge Dislocation in a Model of Alpha-Iron", J. Applied Physics, 42 (1973) 3921.

[4] Kanninen, M. F., "An Analysis of Dynamic Crack Propagation and Arrest for a Material Having a Crack Speed Dependent Fracture Toughness", Prospects of Fracture Mechanics, G. C. Sih, et al, Editors, Noordhoff, Leyden (1974) p 251.

[5] Kanninen, M. F., "A Dynamic Analysis of Unstable Crack Propagation and Arrest in the DCB Test Specimen", Int. J. Fracture, 10 (1974) 415.

[6] Hellen, T. K., "On the Method of Virtual Crack Extension", Int. J. Num. Meth. Eng. 9 (1975) 187.

[7] Hellen, T. K. and Blackburn, W. S., "The Calculation of Stress Intensity Factors for Combined Tensile and Stress Loading", Int. J. Fracture 11 (1975) 605.

[8] Desai, C. S. and Abel, J. F., Introduction to the Finite Element Method, van Nostrand Reinhold Co., New York (1972).

[9] Gaggar, S. and Broutman, L. J., "Crack Growth Resistance of Random Fiber Composites", J. Composite Mat. 9 (1975) 216.

[10] Brinson, H. F. and Yeow, Y. T., "An Investigation of the Failure and Fracture Behavior of Graphite Epoxy Laminates", VPI Report E-75-23, September, 1975.

[11] Rybicki, E. F., "Approximate Three-Dimensional Solutions for Symmetric Laminates Under Inplane Loading", J. Composite Mat. 5 (1971) 354.

[12] Pagano, N. J. and Rybicki, E. F., "On the Significance of Effective Modulus Solutions for Fibrous Composites", J. Composites 8 (1974) 214.

APPENDIX A

FATIGUE-CRACK PROPAGATION IN COMPOSITE MATERIALS

APPENDIX A

FATIGUE-CRACK PROPAGATION IN COMPOSITE MATERIALS

The purpose of this appendix is to inventory existing knowledge on fatigue-crack propagation in composite materials in preparation for treating the analysis of fatigue by means of the mathematical model presented in this report. A brief review of the available literature on the subject is given first. Problems involved in the application of the model will then be discussed.

Literature Review

Characterization of fatigue damage in fiber-reinforced composite materials is complex because of the various damage mechanisms involved, and because of the many material/structural variables in any one composite system. The reported research usually considers only a very limited number of these variables. As a result only fragmentary information is generated. This seriously hampers the development of a fatigue model for composite materials.

The fatigue properties of composites are generally considered to be superior to those of metals. However, it is useful to recognize that this judgment is primarily based on experiments under specific conditions

(a) Mainly unnotched or mildly notched specimens
(b) Small coupons
(c) Primarily unidirectionally reinforced materials
(d) Almost exclusively tension-tension loading.

As an example, consider the fatigue diagram for carbon-fiber reinforced epoxy [1]* in Figure A-1. The maximum stress for the fatigue limit is on the order of the tensile strength, σ_u, as long as no compressive stresses occur (i.e., $R \geq 0$, symbols are defined in the insert to Figure A-1). This means that at a high mean stress, $\sigma_a \simeq \sigma_u - \sigma_m$. For fully reversed loading ($R = -1$), however, the endurance limit is dictated by the compressive strength. The low fatigue properties are associated with fiber buckling [1]. From $R = 0$ to $R = -1$ there is a transition from tensile strength governed fatigue to compressive strength governed fatigue. In this region, fatigue resistance is relatively poor.

* References for this appendix are given on page A-15.

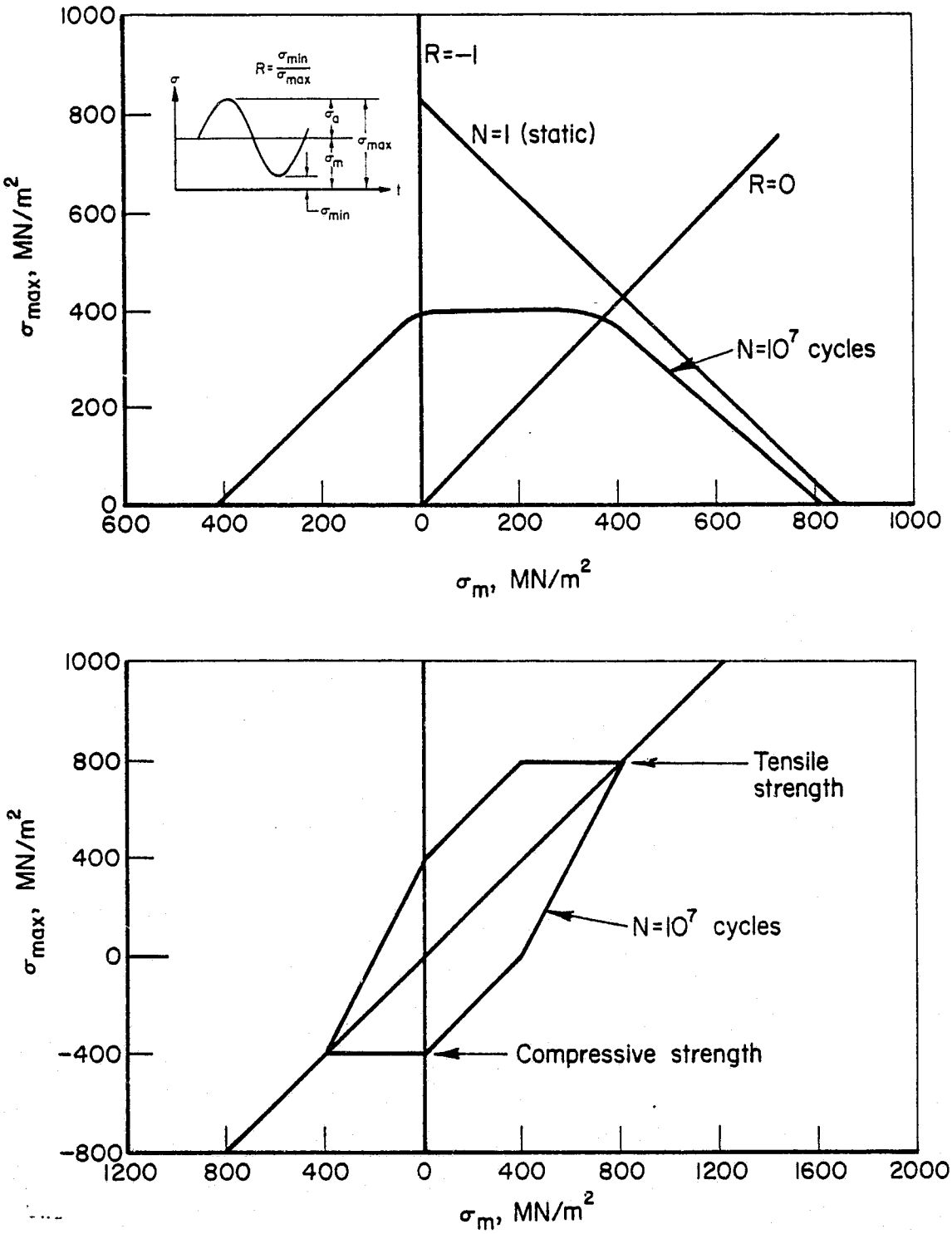

FIGURE A-1. FATIGUE DIAGRAMS FOR CARBON FIBER-EPOXY[1]

The same observations were made for glass-fiber composites [2]. Similarly, fatigue performance is reduced in bending [3] and, in general, in the case of interlaminar shear [1], where other damage mechanisms occur.

The available literature allows an inventory of the various damage mechanisms. These are presented in Table A-1 together with the conditions and the composite systems in which they were observed. The damage mechanisms are

- Fiber-matrix debonding
- Fiber failure (breakage or buckling)
- Matrix cracking
- Delamination.

Intuitively, debonding may be an important damage mechanism in the case of transverse fibers, whereas, fiber breakage may be more important for the case of longitudinal fibers. This is confirmed by the information contained in Table A-1. However, it can be concluded from the table that it is as yet impossible to draw a clear picture of fatigue damage development in composite materials in general.

At this time, an extensive and systematic research program is required to establish a physically sound damage model, capable of showing under which circumstances a particular damage mechanism prevails. An experimental program would require a systematic investigation of all material/structural parameters and loading conditions of a large number of composite systems. One experimental difficulty would be to distinguish between the various damage mechanisms. Newly developed techniques that have been successfully applied to fatigue damage evaluation of composites [10-12], are acoustic emission, time resolved thermography, and tetrabromoethane enhanced X-ray radiography. These techniques could be used in addition to conventional methods to characterize damage development. Then, a general physical model would evolve that is so badly needed as a basis for analytical models.

The fatigue life of metals is terminated by the formation and growth to failure of one or more distinct cracks. In composites on the other hand, a gradual degradation of the specimen is usually observed. Therefore, the end of the fatigue life is often defined as the point where the modulus has decreased a significant amount as a result of wide-spread microdamage. As a result, very little direct quantitative information is available on the growth of cracks during fatigue.

TABLE A-1. FATIGUE DAMAGE DEVELOPMENT

Composite System	Experiments	Fatigue Damage Development	Reference
Glass/Epoxy			
Chopped Strand Mat	Reversed stress unnotched	Debonding followed by matrix cracking	2
Fabric Reinforced and Cross Ply		Debonding of transverse fibers, debonding at yarn cross overs, debonding laminates, resin cracking	2
Unidirectional	Zero-tension	Matrix microcracks, fiber failure	4
Carbon/Epoxy			
Unidirectional	Tension-tension	Fiber failure, matrix cracking	4
	Compression-Compression	Fiber buckling, matrix cracking	1
	Intermediate	Fiber buckling, longitudinal splitting	
Cross Plied	Bending	Debonding, matrix crack, interlamellar crack	
Cross Plied	Bending (notched)	Splitting within and between transverse plies	3
Boron/Epoxy			
Cross Plied	Tension-tension	Strong interface: debonding, fiber failure,	5
	Mildly notched	Matrix cracking: delamination Weak interface: line voids, fiber failure matrix damage	
Boron/Aluminum			
Unidirectional	Tension-tension	Fiber failure, matrix cracking	6

TABLE A-1 (Continued)

Composite System	Experiments	Fatigue Damage Development	Reference
Boron/Aluminum			
Low Angle Cross Plied	Zero-tension	Fiber failure	7
Aluminum/Steel			
Ribbons	Reverse bending	Matrix cracking, debonding, ribbon failure	8
Copper/Tungston			
Unidirectional	Tension-tension	Matrix cracking, fiber failure	9

From a technical point of view, however, the growth of cracks is definitely of interest. In actual structures there will be joints and other local areas of stress concentration. In such areas, fatigue damage will be contained within large undamaged areas. Hence, the local modulus change will not significantly change the stiffness of the component before the fatigue damage develops into large cracks. In such a case, the damage growth may well be totally different from what is observed in a small notched coupon where the damage is not contained.

Apart from the growth of macrocracks, the propagation of microcracks is of interest for the accumulation of fatigue damage in general. It will be the basis for mathematical models for quantitative fatigue evaluation. Yet, only few investigations have been performed to characterize crack growth in composites subjected to cyclic loading.

Fatigue-crack growth in compression (bending) was studied by Kunz and Beaumont [3]. Crack growth showed a retardation period (Figure A-2) which was associated with axial splitting. Mandell and Meier [13] examined crack growth behavior of 0°/90° E-glass-epoxy composite in tension at R = 0. They observed crack extension in small increments. After each increment, the crack was stationary and terminated by a vertical split. After a while, the next ligament (about 0.01 inch in size and containing about 700 fibers) failed.

Here, the information is also quite fragmentary. Crack-growth behavior may be anticipated to depend largely on the composite system and the loading characteristics. For the simple case of unidirectional fibers and tensile loading, the possible crack growth mechanisms are shown in Figure A-3. For multidirectional composites, the sequence of events will be largely complicated by the possibility of delamination and the effect of fiber orientation on debonding.

Modeling Fatigue-Crack Growth

Both fatigue-crack growth in metals and the fracture of low toughness metals can be adequately analyzed with linear elastic fracture mechanics (LEFM). Although there is considerable physical background for the LEFM analysis, the procedure is still entirely pragmatic in its applications. Basically, applied

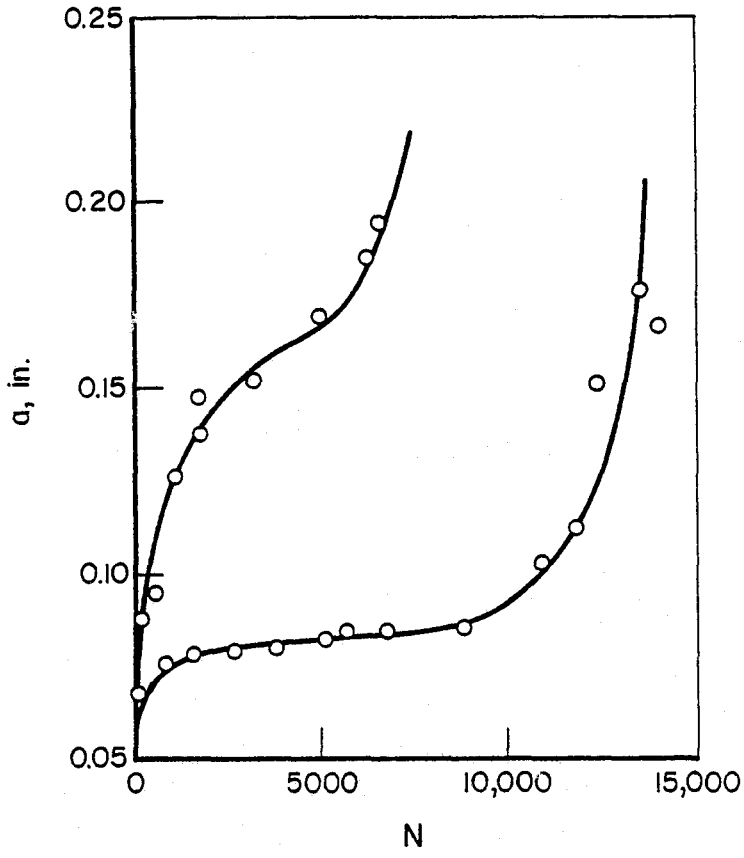

FIGURE A-2. CRACK GROWTH IN COMPRESSION IN U.S. POLYMERIC 702 EPOXY WITH 60 PERCENT UNIDIRECTIONAL (0°) GRAPHITE FIBERS[3]

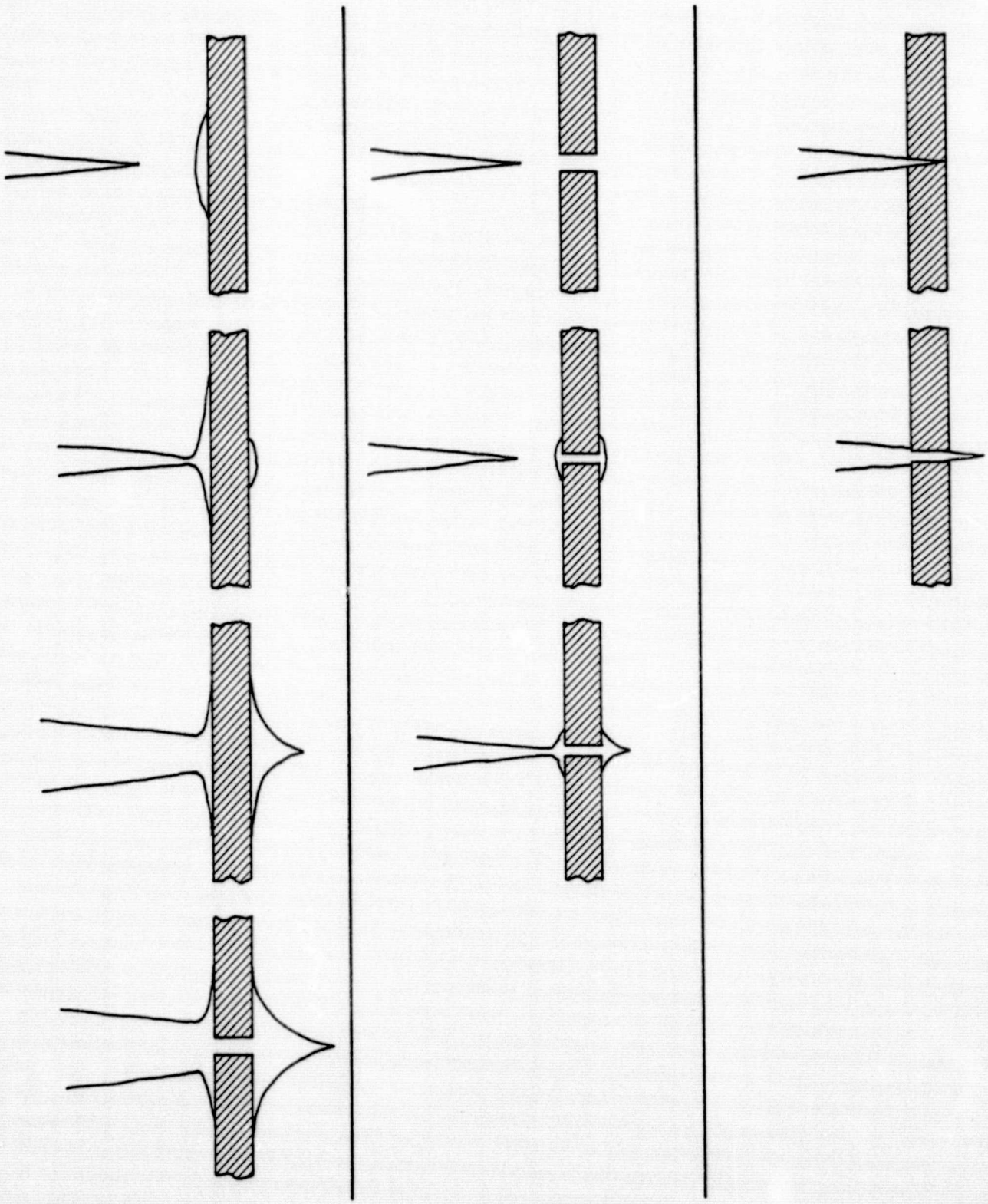

FIGURE A-3. CRACK GROWTH IN UNIDIRECTIONAL COMPOSITE UNDER TENSION

LEFM is nothing more than the recognition that fracture and fatigue-crack growth are governed by the stress-intensity factor. A critical stress-intensity for fracture can be experimentally determined under certain conditions but cannot be derived from theoretical models. Similarly, fatigue-crack growth rates can be measuared as a function of the applied stress intensity, but the form of the relation cannot so far be theoretically predicted.

Physical mechanistic models have been developed for crack growth and fracture in metals (e.g., Reference 14), but mathematical evaluation of these models have failed to provide reliable predictive tools. It was shown only that the stress-intensity factors is a significant parameter in many cases.

The applicability of LEFM in its present state to metals is limited to defects that are large with respect to the structural inhomogeneities. Crack sizes on the order of the size of second phase particles and grains cannot be treated on the basis of the bulk properties. Another restriction to LEFM is that plasticity should be very limited, both with respect to the crack size and the specimen dimension (not only thickness, but also overall size). Plasticity should be fully contained.

Similarly, successful application of LEFM to composites will be limited to cases of large damage, where damage propagation can still be considered to occur in a self-similar fashion. The flaw has to be large with respect to local irregularities in the damage, but small with respect to the specimen dimensions. Therefore, any attempt to correlate small sample data by means of LEFM is basically useless. Nevertheless, numerous publications (e.g., 15 - 20) have appeared on this subject. As might be anticipated, only limited success was achieved. Reasonable correlations on the basis of LEFM could be obtained only in cases where crack extension was fairly regular with one dominating failure mechanism [21-22]. In most cases, the basic assumptions of LEFM had to be mathematically or physically violated to show consistency with experimental data.

Other attempts have been made to derive the fracture behavior by postulating various damage growth mechanisms and then applying fracture mechanics concepts [23-24]. In these cases, the problems are similar to those encountered in the evaluation of micromechanistic crack models in metals. Progress is very slow because the models require so many assumptions and need input quantities that cannot be measured directly.

In view of the foregoing, it is not surprising that very few quantitative models have been proposed to deal with fatigue crack growth in composites. Mandell and Meier [13] presented a mathematical model for the incremental fatigue crack extension observed in their experiments. At each increment of crack growth, the crack extends over a distance defined as the ligament size. Fracture of the ligament was assumed to follow from a Miner's rule linear cumulative damage calculation. The stress history experienced by the ligament basically follows from the elastic crack tip stress field. The stress in the ligament is determined by its distance from the crack tip. Each time the crack advances, the stress increases.

The damage accumulated by the ligament can be determined. This allows calculation of the remaining life when the crack tip has approached the ligament. Then the crack growth rate follows from the assumptions, provided the ligament size is known. The latter has to be found from experiments.

Becasue of its obvious simplicity, the same approach has been proposed many times to treat crack growth in metals. Naturally, it leads to a rising curve, which if properly adjusted will cover a limited collection of data. But, the method has no generality and no predictive power.

Another fatigue crack growth model is based on a static shear lag analysis [28]. In its application to fatigue, the material parameters in this model are changed at the same rate as experimentally observed in a crack growth test. Obviously, the result will be close to the experiments upon which it was based. However, its generality depends upon the generality of the experimental observations.

The energy-based micromechanical analysis scheme described in this report offers more promise for application to growth of fatigue damage. Because it is based on a detailed model of the structural elements in the vicinity of the damage, it requires no advance knowledge of the history and sequence of damage development. What is needed is knowledge of the possible damage mechanisms and of the criteria for their occurrence. A discussion of the utilization of this model for fatigue crack growth will be presented in the following section.

Applicaton of the Present Model to Fatigue

By means of a local energy-based fracture condition, the model can determine the history of damage propagation for various types of local damage. The type and sequence of damage growth that occurs depends upon the energy required by each individual process. In a given location, the type that requires the least energy will occur first. Since the required energy quantities are independent of the geometry and the loading conditions, generality of the model is maintained.

Some problems arising in the applicaton of the model to fatigue can best be explained on the basis of a load displacement diagram as in Figure A-4. For simplicity, linear elastic behavior is assumed. If a crack of size a_1 were to extend to $a_2 = a_1 + \Delta a$ at a load P_1, the energy production (release) rate would be given by triangle OAB. The crack will extend if this energy is equal to or greater than the energy consumption rate for the formation of Δa. If the crack were to extend at a load P_2, the energy-release rate would be given by ΔOCD.

In the case of quasi-static loading, the energy-release rate at crack extension can be directly related to the stress-intensity factor. In fatigue, the load changes cyclicly. The rate of crack growth (in metals) appears to be related to the range of the stress intensity ΔK. Physically, this can be interpreted as the change of crack opening displacement during the cycle. Mathematically ΔK can still be related to a change in energy-release rate ΔG. However, ΔG has no physical meaning. G is the instantaneous value of the energy-release rate at a given crack size and load. If the crack would extend this energy would be available for crack growth. If the crack does not extend no energy is released; the load can be further increased and G attains a different value. Its previous value is of no significance if nothing happened to the crack. As a consequence, the G_{min} at the low point of a fatigue cycle is of no significance for what happens at the maximum stress in this cycle where $G = G_{max}$. Determining $\Delta G = G_{max} - G_{min}$ is then merely a mathematical exercise without physical meaning.

If $da/dn = f(\Delta K)$, where da/dn is the crack growth rate per cycle, one could mathematically write (using $K^2 = EG$)

$$da/dn = f(\sqrt{\Delta G}, \sqrt{G_{max}}) \quad .$$

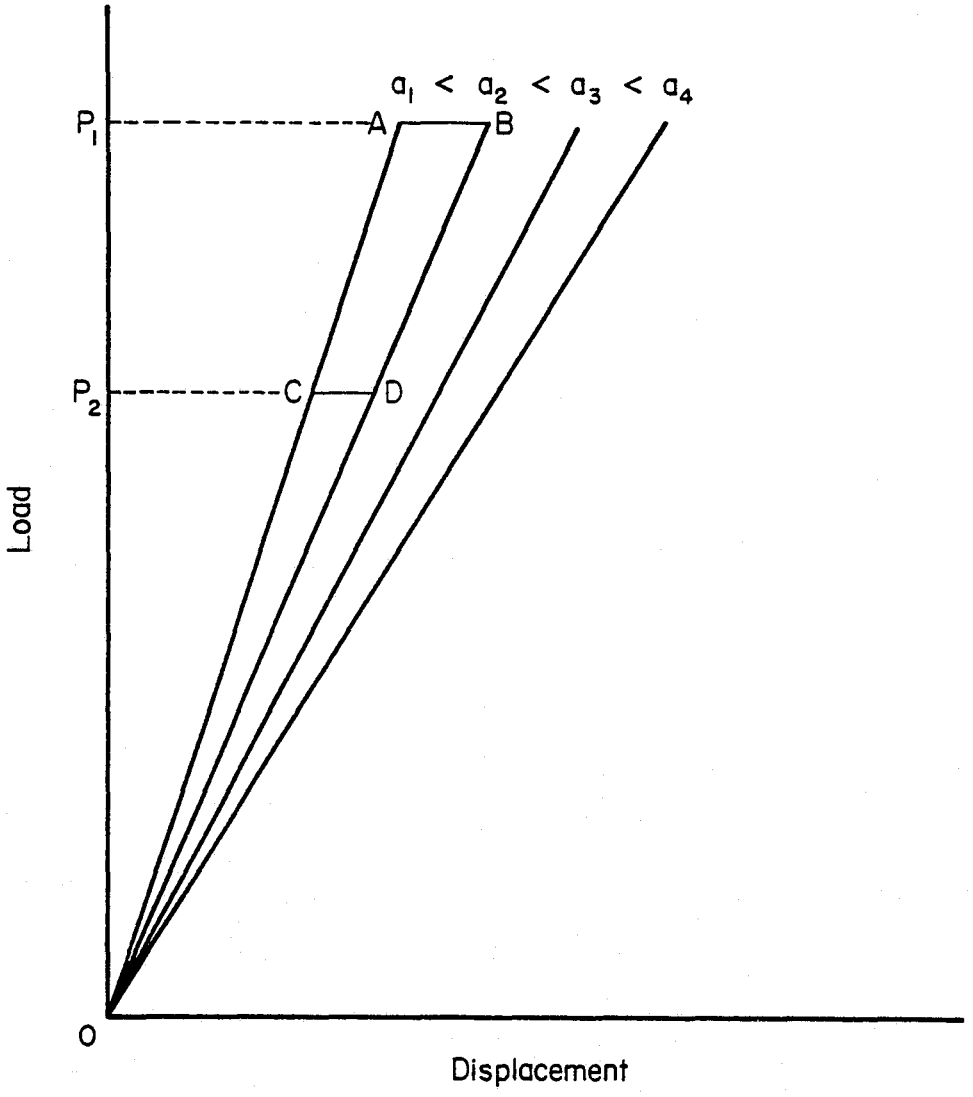

FIGURE A-4. LOAD-DISPLACEMENT DIAGRAM

Figure A-4 shows what this means. If the load is cycled between P_2 and P_1 (Figure A-4), the mathematical representation of ΔG is $\square$ CABD. The phsyical significance of G, however, is limited to the energy released by an instantaneous infinitesimal crack extension.

Crack growth during a cycle can be followed step by step, just as in the case of quasi-static loading. It cannot be based on an integrated release of energy during a cycle unless it is known before hand how damage will develop during the cycle. For this reason, and for the evaluation of the residual stresses built up during unloading, fatigue-damage evaluation would require a cycle-by-cycle exercise of the model. This would be cumbersome. For practical purposes crack extension should be expressible in the parameters descriptive of the fatigue cycle. Therefore, one of the problems to be solved is the establishment of a simplified picture of damage development per cycle. This can be done when sufficient experience is obtained with the model to provide some insight in the mechanics of damage accumulation.

Finally, it might be pointed out that it is possible to evaluate the model experimentally on the basis of real damage observations by means of the techniques described above. Since acoustic emission and thermography are closely related to the energy in the system, they allow a critical evaluation and further development of an energy-release rate model. TBE-enhanced X-ray can be used to characerize the associated damage.

For illustrative purposes consider the case where the energy-release rate can be simply defined on the basis of specimen compliance, C, as

$$G = \frac{1}{2} P^2 \frac{\partial C}{\partial D} \quad ,$$

where P is the applied load and D is a measure of damage size. Experimentally, the compliance is observed [10,12] to be a function of the number of cycles. In crack growth tests on metals, compliance measurements can therefore be used to monitor crack growth. By the same token, compliance measurements can be applied to monitor damage of composites, if the compliance can be characterized as a function of damage. This can be done analytically if the types of damage are identified by means of TBE-enhanced radiography. That is acoustic emission and thermographic measurements are a measure of energy dissipation, and as such, they are a measure of damage accumulation.

Intelligently planned experiments on simple composite configurations can be used to distinguish between each of these quantities. A combination of acoustic emission, thermography and radiography can identify the damage and the associated energy dissipation. Hence, the theoretical model can be substantiated experimentally.

References for Appendix A

[1] Owen, M. J., "Fatigue of Carbon-Fiber Reinforced Plastic Composite Materials", Fracture and Fatigue, Broutman, Editor, Vol. 5, Academic Press (1974), pp 341-359.

[2] Owen, M. J., "Fatigue Damage in Glass-Fiber-Reinforced Plastic Composite Materials", Fracture and Fatigue, Broutman Editor, Vol. 5, Academic Press (1974), pp 313-340.

[3] Kunz, S. C., and Beaumont, P.W.R., "Microcrack Growth in Graphite Fiber-Epoxy Resin Systems During Compressive Fatigue", ASTM STP 569, American Society for Testing and Materials, pp 71-91 (1975).

[4] Dharan, C.K.H., "Fatigue Failure Mechanisms in a Unidirectionally Reinforced Composite Material", ASTM STP 569, American Society for Testing and Materials, pp 171-188 (1975).

[5] Williams, R. S., and Riefsnider, K. L., "Fracture Analysis of Fatigue Damage Mechanisms in Fiber Reinforced Composite Materials Using Scanning Electron Microscopy", Report to AFOSR from Virginia Polytechnic Institute and State University (undated).

[6] Hancock, J. R., "Fatigue of Metal Matrix Composites Materials", Fracture and Fatigue, Broutman, Editor, Academic Press (1974), pp 371-414.

[7] Chamis, C. C., and Sullivan, T. L., "Nonlinear Response of Boron/Aluminum Angleplied Laminates Under Cyclic Tensile Loading: Contributing Mechanisms and Their Effects", ASTM STP 569, American Society for Testing and Materials, pp 95-114 (1975).

[8] Anderson, E., "Fatigue Behavior of Ribbon-Reinforced Composites", Material Science, 8, 676-687 (1973).

[9] Harris, S. J., and Lee, R. E., "Effect of Fiber Spacing on the Fatigue Behavior of Metal Matrix Composites", Composites, pp 101-106 (1974).

[10] Williams, R. S., and Riefsnider, K. L., "Investigation of Acoustic Emission During Fatigue Loading of Composite Specimens", J. Composites Materials, 8, 340-355 (1974).

[11] Williams, R. S., and Riefsnider, K. L., "Real Time Non-Destructive Evaluation of Composite Materials During Fatigue Loading", Virginia Polytechnical Institute, (undated).

[12] Stinchcomb, W. W., Riefsnider, K. L., Marcus, L. A., and Williams, R. S., "Effects of Frequency on the Mechanical Response of Two Composite Materials to Fatigue Load", ASTM STP 569, American Society for Testing and Materials, pp 115-129 (1975).

[13] Mandell, J. F., and Meier, U., "Fatigue Crack Propagation in 0°/90° E-glass/Epoxy Composites", ASTM STP 569, American Society for Testing and Materials, pp 28-44 (1975).

[14] Broek, D., "Elementary Engineering Fracture Mechanics", Noordhoff (1974).

[15] Waddoups, M. E., Eisenmann, J. R., and Kaminski, B. E., "Macroscopic Fracture Mechanics of Advanced Composite Materials", Composite Materials, 5, 466-454 (1971).

[16] Wright, M. A., and Iannussi, F. A., "The Application of the Principles of Linear Elastic Fracture Mechanics to Unidirectional Fiber Reinforced Composite Materials", J. Composite Materials, 7, 430-447 (1973).

[17] Cruse, T. A., "Tensile Strength of Notched Composites", J. Composite Materials, 5, 281-229 (1973).

[18] Gerberich, W. W., "Fracture Mechanics of a Composite with Ductile Fibers", J. Mech. Phys. Solids 19, 71-87 (1971).

[19] Piggott, M. R., "Theoretical Estimation of Fracture Toughness of Fibrous Composites", Materials Science, 5, 669-675 (1970).

[20] Tardiff, G., "Fracture Mechanics of Brittle Matrix Ductile Fiber Composites", Eng. Fract. Mech., 5, 1-10 (1973).

[21] Cooper, G. A., and Kelly, A., "Tensile Properties of Fiber-Reinforced Metals: Fracture Mechanics", J. Mech. Phys. Solids, 15, 279-297 (1967).

[22] Sih, G. C., Chen, E. P., and Huang. S. L., "Fracture Mechanics of Plastic-Fiber Composites", Eng. Fract. Mech., 6, 343-360 (1974).

[23] Marston, T. U., Atkins, A. G., and Felbeck, D. K., "Interfacial Fracture Energy and the Toughness of Composites",J. Mat. Science, 9, 447-455 (1974).

[24] Phillips, D. C., and Tetelman, A. S., "The Fracture Toughness of Fiber Composites", Composites, 216-223 (September 1972).

[25] Beaumont, P.W.R., and Harris, B., "The Energy of Crack Propagation in Carbon Fiber-Reinforced Resin Systems", J. Mat. Science, 7, 1265-1270 (1972).

[26] Cooper, G. A., "The Fracture Toughness of Composites Reinforced with Weakened Fibers", J. Mat. Science, 5, 645-654 (1970).

[27] Lawrence, P., "Some Theoretical Considerations of Fiber Pull-Out From an Elastic Matrix", J. Mat. Science, 7, 1-6 (1972).

[28] Anon., "Fatigue of Notched Composites", Progress Report to NASA from Materials Science Corporation, (May 1974).

APPENDIX B

DISCUSSION OF EXISTING PREDICTIVE TECHNIQUES FOR THE ANALYSIS OF FRACTURE IN COMPOSITES

APPENDIX B

DISCUSSION OF EXISTING PREDICTIVE TECHNIQUES FOR THE ANALYSIS OF FRACTURE IN COMPOSITES

The stress analysis techniques used for designing with composite materials are generally based on the effective modulus representation of fiber-matrix laminates. The effective modulus approach has provided many rules which guide the designer in his selection of lay-up angles and laminate geometries. The designer currently has few such rules to determine the failure point of composite materials, however. In order to use composites to their fullest extent as engineering materials, it will be necessary to establish rational predictive techniques for the various failure modes and, in particular, failure by catastrophic crack propagation.

This appendix contains some background information on failure and strength of composite materials as an aid in placing the fracture model described in this report in proper perspective. A critical review of predictive techniques for fracture of composite materials is also presented for this purpose.

General Discussion on Composite Failure and Fracture

The terms "failure" and "strength" are not always used in a precise manner. There are many different ways that a structure made of a composite material can become unable to adequately perform its primary function. In each such instance, failure is considered to have occurred. The possible failure modes encompass a range of possibilities from simple loss of structural rigidity due to gross inelastic deformation (e.g., yielding) through a reduction in load-carrying capacity due to localized deformation and crack growth (e.g., delamination), to the complete loss of load-carrying capacity by gross macroscopic deformation and separation (e.g., fracture). Failure can be gradual or rapid depending on the nature of the applied loads, the material properties, and the geometry of the structure. For polymer-based composites the load rate, the temperature, environment, and previous load history will also play prominent roles.

Conventionally, the term "strength" is taken to mean the load level at which failure occurs by some means in a standard test specimen. Clearly,

the strength will be a function of many different parameters arising in the test program and may or may not be directly applicable to engineering design situations. It is of great importance that a bridge be established between standard test procedures and engineering applications that will allow accurate reliable estimates of the failure loads to be made in the latter instance using test results (e.g., the yield strength determined in a tension test). Even though substantial failure analysis work has already been performed on composite materials, this capability does not presently exist. Moreover, it appears that the least progress has been made in the most critical problem area--fracture.

Composite fracture research results given in the literature generally fall into one of two broad categories. These are either

(1) A theoretical analysis with the material being treated as a homogeneous but anisotropic linear elastic continuum containing an internal or external flaw of known length, or

(2) a semiempirical analysis of the details of the crack tip region in a unidirectional fiber composite.

The first approach completely ignores the inherently heterogeneous nature of composite materials and the basic way that heterogeneity affects crack extension. In fact, this approach represents only a slight extension of ordinary linear elastic fracture mechanics to account for the anisotropic response of the material to load. In quantitative terms, it involves an evaluation of the left-hand side of the basic fracture mechanics relation for crack growth*

$$G \geq G_c \tag{B-1}$$

with the right-hand side being obtained from experiments. It is this experimental reliance that makes this approach inadequate for fiber composites because, unlike ordinary engineering materials, G_c can be a function of the crack size, shape, and orientation. Because G_c cannot be considered to be a

* The term G denotes the energy released by the structure while G_c denotes the energy dissipated at the crack tip, both per unit area of crack extension.

material constant, the approach is virtually useless for composites except in special circumstances.

The second general approach cited above can also be related to Equation (B-1). It essentially represents a way to determine the right-hand side of (B-1) in terms of basic material properties by considering various mechanisms involved in composite fracture. For example, values of G_c have been deduced for debonding of the fiber from the matrix material, pull-out of the fiber from the matrix, viscoelastic-plastic deformation of the matrix material, etc. While useful, this approach is also an oversimplification for the reasons given above. In addition, in other than simple tests, several of these processes are likely to occur more or less simultaneously with the actual process (and, hence, the amount of energy dissipated) being dictated by the kind and rate of loading, the flaw size and orientation, external geometry, and temperature. Hence, the appropriate value of G_c to be used with a theoretically derived G for a given engineering application cannot be deduced by summing the effects of single mechanisms operating independently. This can contrasted with the simple "rule of mixtures" which works quite well in determining the effective elastic moduli. In contrast to the predictions of effective moduli, where it may be safely assumed that generic stress-strain relations and geometries do not change under load, the prediction of strength implies that processes in the material have progressed to the extent that significant changes in material behavior and geometry have occurred; e.g., yielding, crack formation. Thus, in order to perform a failure analysis, it is necessary to quantify these fundamental changes in the behavior of a structure. While the fundamental changes which take place may be the same for uniaxial composites or multiaxial laminates, failure modes for each can be quite different. The reason is that the local stress state is different even under the same applied loading. The situation is further complicated due to the fact that a simple combination of discrete failure modes does not adequately represent the result in combination.

Micromechanical Failure Processes in Composites

As is the case with homogeneous isotropic materials, it may be safely assumed that failure is precipitated by local defects in a fiber composite. These can occur in the fibers, the matrix, or the interface between the two regions. It has been suggested that a stochastic strength length relationship exists for brittle fibers [1].* That is, the longer the fiber, the greater the probability that a critical defect exists that will cause individual fiber breakage at loads well below the average fiber strength of the composite. After a single fiber break, a crack is induced causing a transfer of load and possibly leading to an avalanche of fiber breakage. Perhaps more importantly, after a fiber breaks, a shear stress is introduced at the fiber-matrix interface and debonding or separation of the fiber and matrix may result. Defects in the matrix may also lead to yielding or actual fracture of the matrix on the local level and thereby create stress concentrations at the fiber or at the fiber-matrix interface. Thus, at relatively low load levels, minute cracks are likely to occur in the fiber, the matrix, or the interface which will be oriented both normal and transverse to the fiber directions. Hence, in some circumstances, the initial crack lengths will be of the same order as the diameter or the distance between fibers.

Even after the microcracks coalesce to form an identifiable separation plane, the size scale of the critical zone of influence near the crack tip will still be of the same order of magnitude as the spacing between fibers. Hence, the same failure mechanisms (e.g., fiber breakage, debonding, and matrix yielding or breakage) will all be important in an overall examination of the fracture process whether the composite is composed of uniaxially or multiaxially oriented fibers.

These failure and/or fracture processes are often described as energy absorption processes. Some of the more prominent energy absorption processes which have been identified with a macrocrack are fiber pull-out, debonding, stress-relaxation, crack bridging, and matrix yielding. Theoretical estimates of the energy absorption per fiber have been compiled by Phillips and Tetelman [2]. They include fiber pull-out, debonding, stress-relaxation, crack bridging, and plastic deformation of the matrix. Brief qualitative descriptions relevant to a macrocrack running transverse to the fibers are as follows.

---

* References for this appendix are given on page B-10.

Figure B-1 shows a possible sequence of events during the fracture of a fiber composite. At some distance ahead of the crack, fibers are intact. In the high stress region near the tip, they are broken; although not necessarily along the crack plane. Immediately behind the crack tip fibers pull-out of the matrix, absorbing energy if the shear stress at the fiber-matrix interface is maintained while the fracture surfaces are separating. Theoretical treatments of the mechanics of the fiber-matrix interface have been given by Cottrell [3], Kelly [6], and by Cooper [7].

In some bonded composites, the stresses near the crack tip could cause the fibers to debond from the matrix before they break. When total debonding occurs, the strain energy in the debonded length of fiber is lost to the material and is dissipated as heat. Fiber stress-relaxation, a variation of the debonding model, estimates the elastic energy that is lost from a broken fiber when the interfacial bond is not destroyed. It is also possible for a fiber to be left intact as the crack propagates. This process, known as crack bridging, can also contribute to the toughness of the material. Analysis of combined debonding and crack bridging for brittle fibers in a perfectly plastic material has been given by Piggott [8].

When brittle fibers are well-bonded to a ductile metal matrix, the fibers tend to snap ahead of the crack tip leaving bridges of matrix material that neck down and fracture in a completely ductile manner. This is also shown in Figure B-1. The fracture toughness in these circumstances is largely governed by the energy involved in the plastic deformation of the matrix to the point of failure. This process has been analyzed by Cooper and Kelly [9].

Of the above energy absorption models, debonding and pull-out have been used most widely. Obviously, the same mechanisms will not be important in all combinations of matrix and fiber materials. For example, the fracture energies of carbon-fiber composites have been more successfully correlated with pull-out model, while for boron and glass composites, debonding is more successful [2]. Marston, et al. [10], however, have shown that no single mechanism such as pull-out, debonding, or stress redistribution taken alone can account for the observed toughnesses of boron-epoxy composites.

Fracture Theories for Composites

Despite the fact that composite materials are by their very nature heterogeneous materials, analyses developed for homogeneous materials are

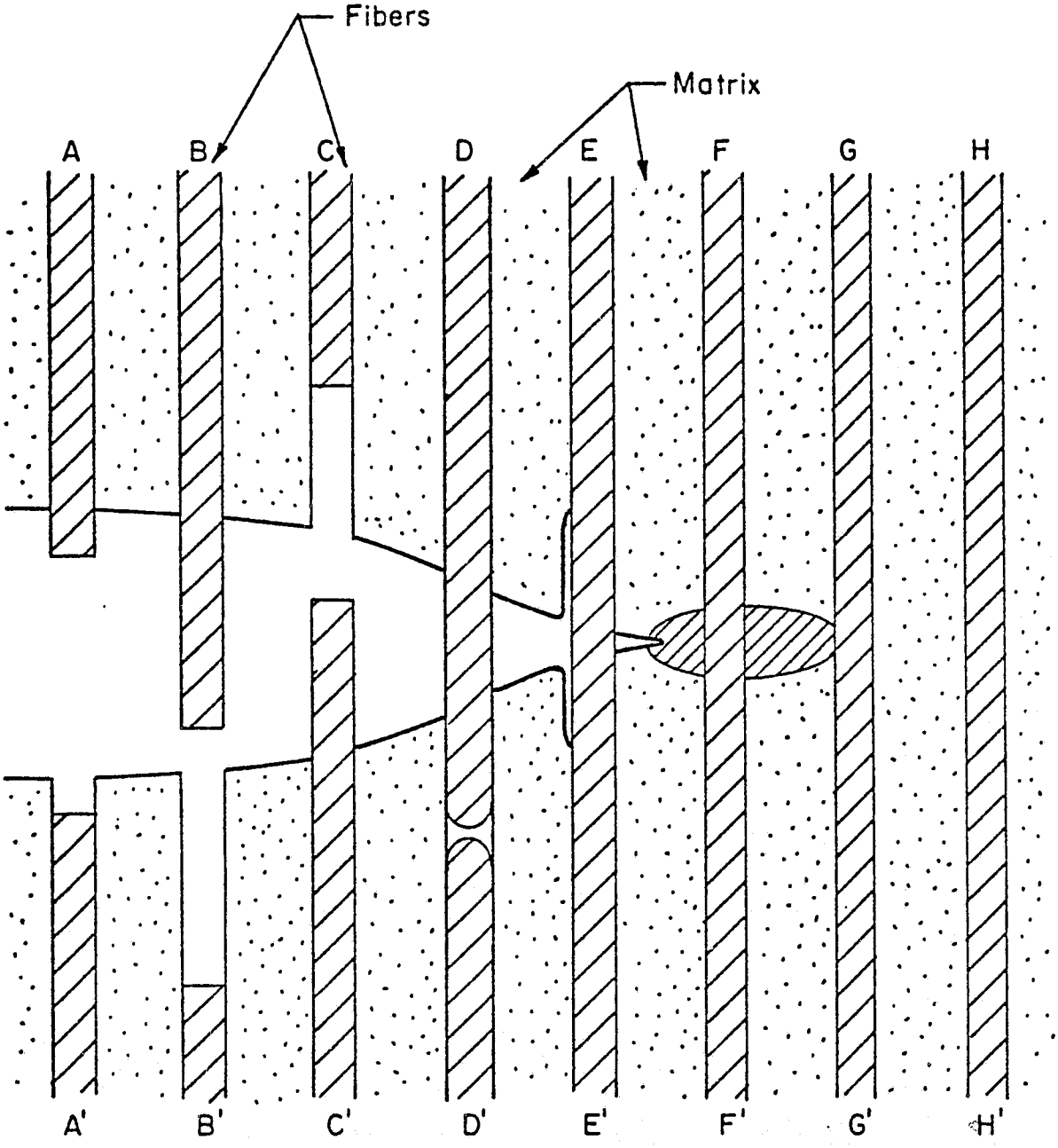

FIGURE B-1. MODEL OF A CRACK TIP IN A FIBER COMPOSITE ILLUSTRATING THE VARIOUS ENERGY DISSIPATION MECHANISMS INVOLVED IN CRACK PROPAGATION

usually applied in treating composite fracture. A typical rationale has been given by Corten [11] by analogy with metals. Correct or not, such a point of view allows relationships between the variables to be developed for engineering purposes that could not otherwise be obtained. This is the basic reason for treating composite fracture with an extension of LEFM to account for their inherent anisotropy.

The applications of fracture mechanics to characterize the failure of composites cannot so far be considered to be particularly successful. There are, in fact, papers in the literature that suggest that some workers do not fully understand the fundamental principles involved. As an example, Waddoups, et al. [12], have employed an empirical extension in linear elastic fracture for isotropic materials which, for a crack of length $2a$ in an infinite body under tensile load normal to the crack, can be expressed as

$$K_I = \sigma \, \pi(\ell + a)^{1/2}$$

where ℓ is taken to be the dimension of a characteristic "intense energy region" at the crack tip. The critical stress for crack extension is then

$$\sigma_c = K_{I_c} / \pi(\ell + a)^{1/2} \quad .$$

Waddoups, et al. treat K_{I_c} and ℓ as disposable parameters which are evaluated from experimental data. They then conclude that the agreement of this equation with the single body of data from which K_{I_c} and ℓ were determined shows that linear elastic fracture mechanics can be applied to composite materials. In fact, they have devised a two-parameter empirical correlation of certain test data which may or may not be applicable to other materials or to other crack orientations in the same material.

A more correct application of anisotropic LEFM to fiber composites is given by Konish, et al. [13]. They noted that critical values of the stress intensity factor for crack growth in the laminates that they tested depended upon the crack path. In particular, a high value of fracture energy was obtained for tests in which fibers were broken while values approximately two orders of magnitude lower were obtained when the crack passed between fibers.

Laboratory results on balanced symmetric laminates containing a flaw perpendicular to direction of loading indicate that the damage mode may propagage in a self-similar manner or may change to another mode; for example, axial splitting. In order to understand fracture of composite materials, it is necessary to develop a mathematical model which will predict and incorporate this nonself similar propagation.

At present, there are a number of fracture theories which attempt to accomplish the above result. Sih [14] and Wu [15] each have theories based on an anisotropic continuum interpretation of fracture. Sih's method is based on a strain energy density concept which will predict not only fracture, but the direction of fracture. This technique requires that the intense energy region size be estimated either from the analysis or an experiment. Wu's method also will predict fracture and the direction of fracture. This is accomplished by locating the intersection of the stress vector surface and the failure surface in the intense energy region ahead of the flaw. Again, the failure surface must be obtained from experimental studies to determine remote properties. In order to use either theory for quantitative comparisons with experiment, the intense energy region ahead of the crack must be observable by experimental techniques.

Another theory due to Kulkarni, et al. [16], uses a materials science approach in which the region adjacent to the notch is modeled as a shear stress transfer region. Here axial fracture (normal to the original crack surface) is assumed. The regions adjacent to the crack are subdivided into a region of shear stress transfer in the core, a region of stress concentration, and region of shear stress transfer in the average material. The quations of analysis are given in Reference [16]. Again, however, the parameter m, which is the number of broken fibers in the core, has to be identified and is determined from laboratory experiments. Thus, for these theories, it appears it is necessary to identify experimentally the size of the region of intense energy adjacent to the flaw and the demarcation between Mode I and Mode II behavior.

In closing this Appendix, it is pointed out that what is needed for the proper utilization of composite materials is a predictive capability for

composite fracture that can take account of loading and geometry of the structure, environmental effects, as well as the properties of the composite's constitutents and its microstructural design. This report describes an approach to seek this end by, in essence, unifying the two current approaches in composite materials. This is accomplished by treating the material as heterogeneous where microstructural effects are predominant and as homogeneous and anisotropic only where it is appropriate to do so.

References for Appendix B

[1] Rosen, B. W., "Tensile Failure of Fibrous Composites", AIAA Journal, 2, 1965 (1964).

[2] Phillips, D. C., and Tetelman, A. S., "The Fracture Toughness of Fiber Composites", Composites, 3, 216 (1972).

[3] Cottrell, "Strong Solids", Roy. Soc. Proc. A282, 2, (1964).

[4] Cooper, G. A., and Kelly, A., "Role of the Interface in the Fracture of Fiber-Composite Materials", ASTM STP 452, p 90 (1969).

[5] Greszczuk, L. B., "Theoretical Studies of the Mechanisms of the Fiber-Matrix Interface in Composites", ASTM STP 452, p 42 (1969).

[6] Kelly, A., "Interface Effects and the Work of Fracture of a Fibrous Composite", Proc. Royal Soc. A319, 95 (1970).

[7] Cooper, G. A., "The Fracture Toughness of Composites Reinforced with Weakened Fibers", J. Mat. Sci., 5, 645 (1970).

[8] Piggott, M. R., "Theoretical Estimation of Fracture Toughness of Fibrous Composites", J. Mat. Sci., 5, 669 (1970).

[9] Cooper, G. A., and Kelly, A., "Tensile Properties of Fiber-Reinforced Materials: Fracture Mechanics", J. Mech. Phys. Solids 15, 279 (1967).

[10] Marston, T. U., Atkinson, A. G., and Felbeck, D. K., "Interfacial Fracture Energy and the Toughness of Composites", J. Mat. Sci. 9, 447 (1974).

[11] Corten, H. T., "Fracture Mechanics of Composites", Fracture, Vol. VII, H. Liebowitz (editor), Academic Press, New York, p 676 (1972).

[12] Waddoups, M. E., Eisenmann, J. R., and Kaminski, B. E., "Macroscopic Fracture Mechanics of Advanced Composite Materials", J. Comp. Mat. 5, 466 (1971).

[13] Konish, H. J., Swedlow, J. L., and Cruse, A. T., "Fracture Phenomena in Advanced Fiber Composite Materials", AIAA Journal 11, 40 (1973).

[14] Sih, G. C., and Chen, E.P., "Fracture Analysis of Unidirectional Composites", J. Comp. Mat'ls., Vol. 7, (April 1973), p. 230.

[15] Wu, E. M., "Strength and Fracture of Composites", Composite Materials, Broutman, L. J., and Krock, R. H., Ed's., Vol. 5, Fracture and Fatigue, Broutman, L. J., Ed., Academic Press, N. Y., (1974).

[16] Kulkarni, S. V., and Rosen, B. W., "Design Data for Composite Structure Safelife Prediction: Analysis Evaluation", Materials Science Corporation, TFR/2221, (August 1973).